FIZIOLOGIA
physiology

ACCREDITED BY CNCSIS - B+CATEGORY ■ CODE 240

http://www.ebscohost.com/titleLists/a9h-journals.pdf

Fiziologia (Physiology) is issued quarterly
Printed at Editura **EUROSTAMPA**
www.eurostampa.ro
Bd. Revoluţiei din 1989 nr. 26, Timişoara
Tel/fax: 0256-204816
ISSN 1223-2076

Instructions to Authors

Submission: Only original papers in English are considered and should be sent to the following address: carmen.tatu@umft.ro

Manuscripts should be submitted by e-mail only, written in Microsoft Word 97 or later versions.

Conditions: All manuscripts are subject to editorial review. Manuscripts are received with the explicit understanding that they are not under simultaneous consideration by any other publication. Submission of an article for publication implies the transfer of the Copyright from the author the publisher upon acceptance. Accepted papers become the permanent property of "Fiziologia" (Physiology) and may not be reproduced by any means, in-whole or in part, without the written consent of the publisher. It is the author's responsibility to obtain permission to reproduce illustrations, tables, etc. from other publications.

Arrangement:

Title page: The first of each paper should indicate the title, the authors' names and their affiliation(s). A short title for use as running head is also required.

Keywords: for indexing purposes, a list of 3-5 keywords in English and Romanian is essential.

Corresponding author: Indicate the full name, the email address and the phone number.

Abstract: Each paper needs abstract and title in Romanian and English language, fonts size 9, Arial Narrow.

Body text: fonts size 10, Arial Narrow.

Small type: Paragraphs which can or must be set in smaller type (case histories, test methods, etc.) should be indicated with a „p" (petit) in the margin on the left-hand side.

Footnotes: Avoid footnotes. When essential, they are numbered consecutively and typed at the foot of the appropriate page, fonts size 8, Arial Narrow.

Tables and illustrations: Tables (numbered in Roman numerals) and illustrations (numbered in Arabic numerals) should be prepared on separate sheets, fonts size 9, Arial Narrow. Tables require a heading, and figures a legend, also prepared on a separate sheet. For the reproduction of illustrations, only good drawings and original photographs can be accepted; negatives or photocopies cannot be used. When possible, group several illustrations on one block for reproduction (max. size 140x188 mm) or provide crop marks. On the back of each illustration indicate its number, the author's name, and article title.

References: In the text identify references by Arabic figures, (in brackets), fonts size 9, Arial Narrow. Material submitted for publication but not yet accepted should be noted as "unpublished data" and not be included in the reference list. The list of references should include only those publications which are cited in the text. The references should be numbered and arranged alphabetically by the authors' names. The surnames of the authors followed by initials should be given. There should be no punctuation signs other than a comma to separate the authors. When there are more than 3 authors, the names of the 3 only are used, followed by "et al" abbreviate journal names according to the Index Medicus system. (also see International Committee of Medical Journal Editors: Uniform Requirements for manuscripts submitted to biomedical journals. Ann Intern Med 1982; 96: 766-771).

Examples:

(a) Papers published in periodicals: Kauffman HF, van der Heide S, Beaumont F, et al: Class-specific antibody determination against Aspergillus fumigatus by mean of the enzyme-linked immunosorbent assay. III. Comparative study: IgG, IgA, IgM, ELISA titers, precipitating antibodies and IGE biding after fractionation of the antigen. Int Arch Allergy Appl Immunol 1986; 80:300 - 306.

(b) Monographs; Matthews DE, Farewell VT: *Using and Understanding Medical Statistics.* Basel, Karger, 1985.

(c) Edited books: Hardy WD Jr, Essex *M:. FeLV-inducted feline acquired immune deficiency syndrome: A model for human AIDS;* in Klein E(ed): Acquired Immunodeficiency Syndrome. Prag Allergy, Busel, Karger, 1986, vol 37,353 - 376.

Galley proofs: unless indicated otherwise, galley proofs are sent to the first-named author and should be returned with the least possible delay. Alternations made in galley proofs, other than the corrections of printer's errors, are charged to the author. No page proofs are supplied.

CONTENTS

CUPRINS

EXPERIMENTAL ELECTROPHYSIOLOGICAL DEVICE FOR THE APPRECIATION OF THE CARDIAC SYSTOLIC FUNCTION – A PILOT STUDY

VALENTIN ORDODI[1,2], LILIANA MÂȚIU-IOVAN[1], GRETA BĂRBULESCU[2,3], DANIEL BONCIOG[1], DACIANA NISTOR[2,3], DANIELA CRÎSNIC[2,4], GABRIELA TĂNASIE[2,3]

[1] Politehnica University of Timișoara, 2 Victoriei Square, RO-300006, Timișoara, România
[2] OncoGen Research Center, Pius Bânzeu Clinical Emergency Hospital, 156 Liviu Rebreanu Bv, RO-300723, Timișoara România
[3] University of Medicine and Pharmacy "Victor Babeș" Timișoara, 2 Eftimie Murgu Square RO-300041, Timișoara, România
[4] SC Biodim SRL, 59 Porumbescu St, RO-300239, Timișoara, România

ABSTRACT
In this paper we propose the design and implementation of an electrophysiological experimental device capable of acquiring in real time three cardiovascular parameters: an electrocardiographic derivation (DII), the phonocardiogram and the peripheral photoplestismogram pulse wave at the level of a finger from the upper limb. These parameters allow us to measure systolic parameters with the help of appropriate software and mathematical relationships to calculate the Blumberger hemodynamic index and ejection fraction of the left ventricle. The method is completely noninvasive, simple to perform than the classic polyphysiogram that involved recording the carotid sphygmogram and allows the assessment of the systolic function of the left ventricle in the family doctor's office or of general medicine that does not have the equipment and skills necessary to perform the echocardiographic examination. The preliminary results show a good correlation between the ejection fraction measured echocardiographically (72%) and the value determined with the presented device (77%), which recommends testing the device on significant batches of patients with various cardiovascular pathologies.
Keywords: electrophysiological, non-invasive, cardiac systolic function

INTRODUCTION

Hypertensive, ischemic and valvular cardiovascular pathology is currently the most important cause of morbidity and mortality worldwide and the age of onset of these diseases is increasingly reduced. The instrumental exploration of the cardiovascular function is a stage of maximum importance for specifying a correct diagnosis, respectively prescribing the appropriate treatment. The range of investigations that can explore the cardiovascular system is extremely extensive due to the development of electronics, computers and computers, biophotonics, imaging, etc. In addition to modern imaging techniques: echocardiography, coronarography, radioisotopic exploration of cardiac and pulmonary function, computer tomography and nuclear magnetic resonance, the traditional methods: electrocardiography, phonocardiography and photoplethysmography are widely available which provide important data for an accurate cardiological diagnosis. Heart failure is a syndrome that occurs during many ischemic or non-ischemic heart conditions. Left and congestive heart failure are more commonly encountered in medical practice compared to isolated right heart failure.

The assessment of the systolic-diastolic function of the left ventricle and of the heart as a whole is performed at the present time with high accuracy using echocardiography. The left ventricle is considered to have normal systolic function if the ejection fraction is greater than 50% and if its volume index is below 97 ml / m2 body surface area.

Systolic times are defined as the durations of the various phases of ventricular systole. They are important markers in the evaluation of cardiac performance, which can be determined simply, quickly and noninvasively with the help of the polyphysiogram. Traditionally, three parameters are recorded simultaneously: ECG, phonocardiogram and carotid artery pulse (Figure 1):

Received September 20th 2019. Accepted November 24th 2019. Address for correspondence: Valentin Ordodi, PhD, Politehnica University of Timișoara, 2 Victoriei Square, RO-300006, Timișoara, România; phone: +40-256-404219; e-mail: vali.medtm99@gmail.com

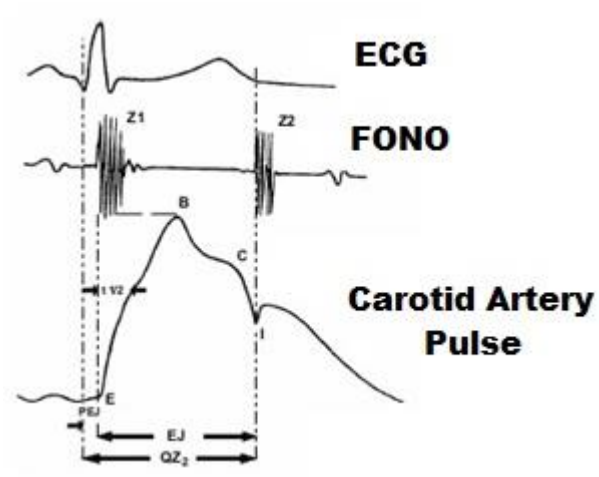

Fig. 1. The classic polyphysiogram. Systolic times. (According to Dan Dobreanu UMF Tg Mureș)

Usually the following systolic times are determined:

a) Electromechanical systole (QZ2). It is measured from the beginning of the Q wave on the electrocardiogram and up to the beginning of the second noise on the phonocardiogram.

b) The ejection period (EJ) is measured on the carotid sphygmogram. It is measured from the base of the anacrotic wave to the dichroic incision.

c) The pre-ejection period (PEJ) represents the difference between the electromechanical systole and the ejection period.

If contractile dysfunction of the left ventricle appears, there is an increase in pre-ejection duration (PEJ) and a reduction in ejection duration (EJ) with relatively unchanged electromechanical systole (QZ2) duration. The Blumberger hemodynamic index can be defined as:

$$Blumberger\ hemodynamic\ index = \frac{EJ}{PEJ}$$

Where:
- EJ - ejection period (s)
- PEJ - pre-ejection period (s)

This parameter more accurately assesses the systolic dysfunction of the left ventricle compared to the two parameters considered separately.

Using systolic times we can calculate the ejection fraction of the left ventricle (Fej) using the relation:

$$F_{ej} = (\ 1.125 - 1.350 \cdot \frac{PEJ}{EJ}\ ) \cdot 100$$

Where:
- EJ - ejection period (s)
- PEJ - pre-ejection period (s)

EXPERIMENTAL DEVICE

The experimental device acquires, amplifies, processes and displays simultaneously the following biosignals generated during heart activity: cardiac electrical activity (electrocardiogram) by recording with surface electrodes, using the standard bipolar derivatives of the limbs, the phonocardiogram is recorded in the mitral, erb or aortic area and photopletismogram generated by the pulse wave, recorded at the level of a finger by the hand by the technique of reflection of the light radiation on the surface of the skin.

The experimental device (Figure 2) contains three main parts:

- The acquisition and amplification module of the electrical and mechanical signals generated during the cardiac revolution
- The power supply of the amplifier for the phonocardiogram
- Analog-numerical conversion module of these signals as well as the interface with the computer (Arduino UNO R3 acquisition board)

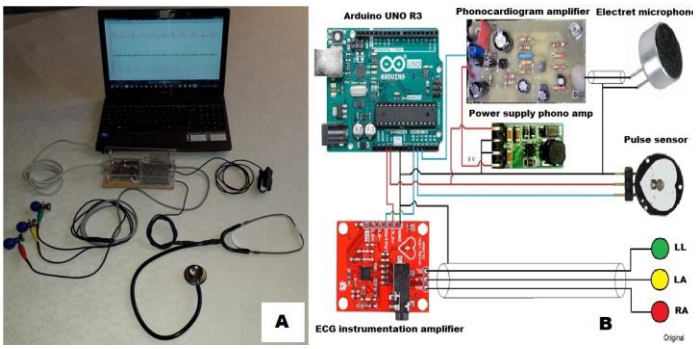

Fig. 2. The experimental device - overview (2A), respectively block diagram (2B).

The ECG module uses an integrated AD8232 instrumentation amplifier produced by Analog Devices. It is designed for recording a single bipolar ECG derivation, the configuration used in the experimental device uses the D_{II} derivation because in most individuals the amplitude of the waves in this derivation is maximum (the projection of the cardiac electric vector in the Einthoven triangle). The ECG module uses an integrated AD8232 instrumentation amplifier produced by Analog Devices. It is designed for recording a single bipolar ECG derivation, the configuration used in the experimental device uses the D_{II} derivation because in most individuals the amplitude of the waves in this derivation is maximum (the projection of the cardiac electric vector in the Einthoven triangle). The block

diagram of this circuit is shown in figure 3A. The acquisition of ECG biopotentials was performed using suction-type electrodes attached to the root of the upper limbs (right and left) and to the root of the lower left limb in accordance with the standard bipolar limb derivatives. The conventional colors for the electrodes were observed. The connection cable between the electrodes and the ECG amplifier is shielded to prevent the penetration of electromagnetic parasites.

The audio frequency amplifier for the phonocardiogram uses a simple transistor amplifier schematic with three transistors adapted for the electret microphone. The device contains a "low down" filter to mitigate parasitic noise from the outside environment. Figure 3B shows the principle diagram of this amplifier. For the acquisition of cardiac sounds, a common stethoscope was used, which was adapted to the electret microphone (Figure 3C). The connection between the microphone and the amplifier was made through a well-shielded audio cable. Since the amplifier for phonocardiography requires a supply voltage of + 9V, it was necessary to include a booster voltage regulator from + 5V to + 9V. Figure 3D shows the principle diagram of the device.

The instrumentation amplifier for recording the electrocardiogram and the audio frequency amplifier for the recording of the phonocardiogram are mounted shielded in Faraday cages to be protected from electromagnetic interference.

The photoplethysmograph (Figure 3E) used to detect the volume variation synchronous with the cardiac activity of a finger from the upper limb was used an optical sensor based on the principle of light ray reflection on the surface of the tegument. This sensor has included the amplification module so that the useful signal is obtained directly at the output. The sensor was included in the housing of a common defective pulseoximetry sensor. The connection with the acquisition board was made by shielded cable which also ensures the + 5V supply of the module.

Acquisition board Arduino UNO R3 (Figure 3F) provides interface with the computer, respectively the analog-digital conversion of the biosignals from the patient. It is a flexible structure, programmable in C ++ and upload in Arduino IDE, provided with a USB port that allows connection to any computer.

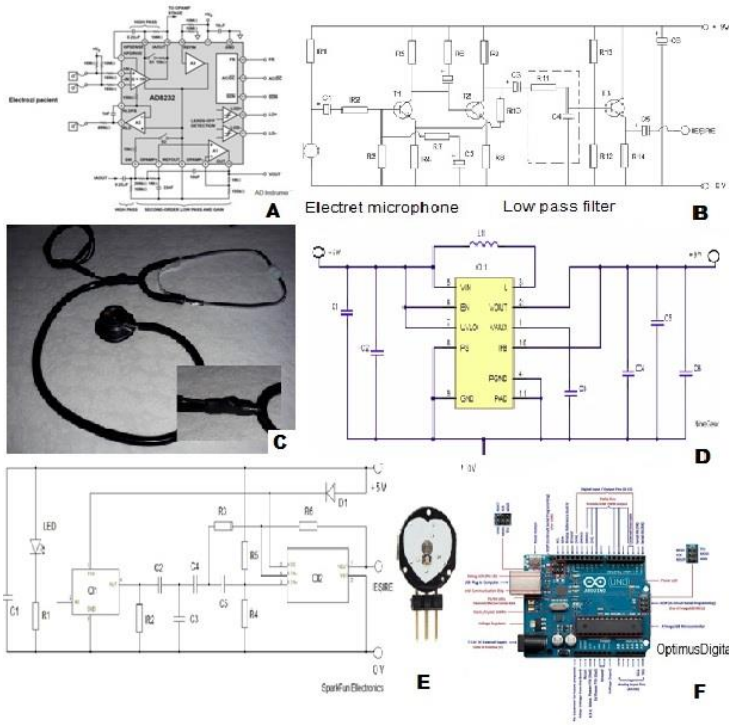

Fig. 3. The modules of the experimental device. A – ECG instrumentation amplifier block diagram, B – phonocardiogram amplifier principle diagram, C – modified stethoscope with electret microphone, D – power supply for phonocardiogram amplifier principle diagram, E – photopletismograph principle diagram and overview, F – Arduino UNO R3 data board overview.

For all data acquisition we used ”Serial Oscilloscope” open source software.

RESULTS AND DISCUSSION – CASE STUDY

A preliminary experiment using the proposed experimental device was performed on a male subject 44 years old, without cardiovascular pathology evaluated cardiologically. Echocardiography determines the ejection fraction = 72%.

The signal acquisition was made in clinostatism, in a room with a temperature of 22^0 C, after a rest of 10 minutes under the usual conditions of any routine electrocardiographic examination. For the electrocardiogram the bipolar derivation of the D_{II} was chosen, the phonocardiogram was recorded by placing the stethoscope in the Erb area, and the photoplethysmogram was recorded at the level of the left hand index.

Previously blood pressure was measured by listening method and a standard electrocardiogram was recorded with electrocardiograph Innomed HS80G – L.

The recording of the biosignals and the marking of the systolic times is shown in Figure 4.

Fig. 4. Experimental polyphysiogram. Systolic times.

Since all the parameters that enter into the calculation equations have the same units of measurement and are used as mathematical (dimensionless) reports we can measure directly on the record in mm, these sizes. Thus we will have:

- QZ2 (electromechanical systole) = 25.8 mm
- EJ (ejection period) = 20.5 mm

We calculate the PEJ (pre-ejection period) with the relation:

$$PEJ = QZ_2 - EJ = 25{,}8\ mm - 20{,}5\ mm = 5{,}3\ mm$$

Knowing these data we can calculate the Bumberger hemodynamic index and ejection fraction (F_{ej}) with the formulas:

$$\textit{Blumberger hemodinamic index} = \frac{EJ}{PEJ} = \frac{20{,}5}{5{,}3} = 3.86$$

$$F_{ej} = \left(1.125 - 1.350 \cdot \frac{PEJ}{EJ}\right) \cdot 100 = \left(1.125 - 1.350 \cdot \frac{5{,}3}{20.5}\right) \cdot 100$$

$$F_{ej} = 77\ \%$$

Table I presents the experimental data obtained in the case study:

Table I. Case Study. Experimental data.

Parameter	Echocardiography	Experimnetal device	Normal value
Blumberger hemodinamic index	-	3.86	2.5 - 5
Ejection fraction (%)	72	77	>50

CONCLUSION

The case study shows that the proposed working hypothesis is correct and can be carried out to carry out extensive studies on batches of patients that reach the statistical significance for each type of pathology, so that the experimental device and the working method can be validated.

REFERENCES

1. Bunu C. Fiziologia aparatului cardiovascular. Ed. Orizonturi Universitare, Timișoara, 2003.
2. Noveanu L, Mihalaș G. Fiziologie Practică. Vol II. Ed. Mirton Timișoara, 2005.
3. Tănăsie G et al. Fiziologie Aplicată. Demonstrații și explorări peu medicina dentară. Ed. Mirton Timișoara, 2006.
4. Noveanu L et al. Suport de lucrări practice de fiziologie pentru balneofiziokinetoterapie. Ed. Mirton Timișoara, 2006.
5. Diaconu C. Explorări funcționale în medicina internă. Ed. All, București, 2016.
6. Ordodi LV, Păunescu V, Mic AA, Ionac M, Săndesc D, Mic FA. A small scale oxygenator for cardiopulmonary bypass in rats. *The International Journal of Artificial Organs* 2006, 29(8).
7. Ordodi VL, Paunescu V, Ionac M, Sandesc D, Mic AA, Tatu CA, Mic FA. Artificial device for extracorporeal blood oxygenation in rats. *Artif Organs.* 2008; 32(1): 66-70.
8. Ordodi LV, Mic AF, Mic AA, Toma O, Săndesc D, Păunescu V. A simple device for invasive measurement of arterial blood pressure and ECG in the anesthesized rat. *Timisoara Medical Journal* 2005; 55(3).
9. Arduino - Introduction. arduino.cc.
10. Toma IC, Gui V, Otesteanu M. Dispozitive si circuite electronice. Partea a II-a. Circuite electronice. Institutul Politehnic "Traian Vuia" Timisoara, Facultatea de Electrotehnică, 1984.
11. Savu T. Sisteme computerizate pentru achiziția de date. Îndrumar de laborator; București, 1999.
12. Popa M. Microprocesoare şi microcontrolere, Ed. Politehnica, Timişoara, 1997.
13. www.arduino.cc/en/uploads/Main/Arduino_Uno_Rev3-schematic.pdf
14. Summers L. Using buttons and switches with an Arduino. 2014 [online] connectedly.com. Available at: http://www.connectedly.com/using-buttons-and-switches-arduino
15. Bacivarof IC. Conexiuni prin lipire in aparatura electronica, Editura Tehnica Bucuresti, 1984.
16. Nowichi JR., Power supplies for electronic equipment, London, 1971.

DISPOZITIV EXPERIMENTAL ELECTROFIZIOLOGIC PENTRU EVALUAREA FUNCȚIEI SISTOLICE CARDIACE – STUDIU PILOT

REZUMAT

În lucrarea de față ne propunem proiectarea și realizarea unui dispozitiv experimental electrofiziologic de tip polifiziograf capabil să achiziționeze în timp real trei parametrii cardiovasculari: o derivație electrocardiografică (DII), fonocardiograma și fotoplestismograma periferică la nivelul unui deget de la membrul superior. Acești parametri ne permit să măsurăm timpii sistolici și cu ajutorul unui software adecvat și a unor relații matematice să calculăm indicele hemodinamic Blumberger și fracția de ejecție a ventriculului stâng. Metoda este complet noninvazivă, mai simplu de executat decât polifiziograma clasică care presupunea înregistrarea sfigmogramei carotidiene și permite aprecierea funcției sistolice a ventriculului stâng în cabinetul medicului de familie sau de medicină generală care nu posedă echipamentul și competențele necesare efectuării examenului ecocardiografic. Rezultatele preliminare arata o bună corelație între fracția de ejecție masurată ecocardiografic (72%) și valoarea determinata cu dispozitivul prezentat (77%), fapt care recomanda testarea dispozitivului pe loturi semnificative de pacienti cu diverse patologii cardiovasculare.

Cuvinte cheie: electrofiziologic, noninvaziv, funcția sistolică cardiacă.

MODERN APPLICATION OF NEXT-GENERATION SEQUENCING (NGS)

LAURA POPA, DANIELA CRISNIC, DACIANA NISTOR, PLESCA DANA, CARMEN TATU, GABRIELA TANASIE, ROXANA ZOGOREAN, OANA GAVRILIUC, SIMONA ANGHEL, FLORINA BOJIN, VIRGIL PAUNESCU

Clinical Emergency County Hospital "Pius Brinzeu" Timisoara, Centre for Gene and Cellular Therapies in Cancer Treatment - OncoGen
Department of Functional Sciences, "Victor Babes" University of Medicine and Pharmacy Timisoara

ABSTRACT

DNA sequencing refers to determine the correct order of nucleotide bases in a DNA macromolecule using sequencing machines. The first sequencing method based on enzymatic synthesis or Sanger method, opened the way in revolutionizing the field of genomics and other scientific fields.

Over the past ten years, massively parallel DNA sequencing platforms were released. The appearance on Next Generation Sequencing has changed the view of the analysis and understanding of living bodies. The progress accelerated biological and biomedical research by bringing together the DNA sequencing, epigenetic sequencing, fragment analysis, genotyping and genomic profiling. Longer read lengths, shorter time to result also a lower overall cost of DNA sequencing, made it widely accessible and more efficient.

In this review, we present a brief evolution of sequencing methods from the beginning to nowadays and the board range of applications for NGS technologies.

Keywords: DNA, sequencing, Sanger method, molecules, nucleotides

INTRODUCTION

Genetic sequencing or DNA sequencing refers to any method or technology that is used to determine the order of the four bases: adenine (A), guanine (G), cytosine (C) and thymine (T) - in a DNA strand. Being able to read the order of nucleic acid is our opportunity to uncover the hereditary and biochemical properties of terrestrial life **[1].**

At the present time there are several sequencing methods, ranked according to when they were discovered, in classical or first generation methods and second generation (next generation) methods. The first category is represented by the chemical method of Maxam and Gilbert and the enzymatic method also called Sanger method which is based on enzymatic synthesis. The next generation of sequencing, also known as high-throughput sequencing uses modern technologies, represented by Illumina (Solexa) sequencing, Roche 454 sequencing and Ion Torrent Proton / PGM sequencing.

Deoxyribonucleic acid (DNA) was demonstrated as the genetic material by Oswald Theodore Avery in 1944 **[2].** In 1953 James Watson and Francis Crick have published their latest discovery: the molecular structure of DNA- the double helix **[1, 3].** Their discovery was based on Rosalind Franklin and Maurice Wilkins' X-ray diffraction of DNA. In 1962 Watson, Crick and Wilkins shared the Nobel Prize in Medicine.

Robert Holley and colleagues were able to produce the very first whole nucleic acid sequence, that of alanine tRNA from Saccharomyces cerevisiae in 1965. Robert William Holley was awarded with the Nobel Prize in 1968 for describing the structure of alanine transfer RNA, linking DNA and protein synthesis **[4].**

The methods of determining the nucleotide sequence of DNA fragments were discovered in 1970, independently by Walter Gilbert (the chemical degradation technique) and Frederick Sanger (the enzymatic synthesis technique). Both Gilbert and Sanger were awarded with the Nobel Prize for Chemistry in 1980 [**5]**.

The first whole genome of an organism, the virus Phange-Phi X174, was sequenced in 1977. In 1988, The Human Genome Project began, and it was completed in 2003.

Received September 16th 2019. Accepted November 20th 2019.

Address for correspondence: Laura Popa, MD, Clinical Emergency County Hospital "Pius Brînzeu" Timișoara, Centre for Cellular and Gene Therapies in the Treatment of Cancer – OncoGen; Liviu Rebreanu Street No. 156, RO-300723, Timisoara, Romania; phone: +40743129395; e-mail: laura.claudia21@yahoo.com

The chemical degradation sequencing technique

In the chemical DNA sequencing method end-labelled DNA is partially cleaved at each of the four nucleotide bases in four different reactions. The fragments are ordered by size by gel electrophoresis and the sequence read-off an autoradiograph by noting which base-specific agent cleaved at each successive nucleotide along the strand **[6].**

Chemical method uses chemicals to break the DNA molecules into certain nucleotides. After marking the heads 5` with 32P, the sequenced DNA is distorted (it becomes a single-wire) and is divided into four samples. Each of the four samples is treated (with piperidine) to produce ruptures at nucleotides with specific bases that are also chemically modified in a certain way. The conditions are so regulated that the ruptures cannot occur to all nucleotides in such a fragment that populations are obtained of different fragment sizes for each sample, some marked at the end 5`. The fragments are separated by electrophoresis and are identified by autoradiography. The autoradiograph is a polyacrylamide gel, where the nucleotides are displayed from the site of label. This method was used to sequence oligonucleotides (short nucleotide polymers, usually smaller than 50 base-pairs in length)**.** Molecules labeled at the 3' end can be sequenced up to 100-200 bases from the labeled termination **[7].**

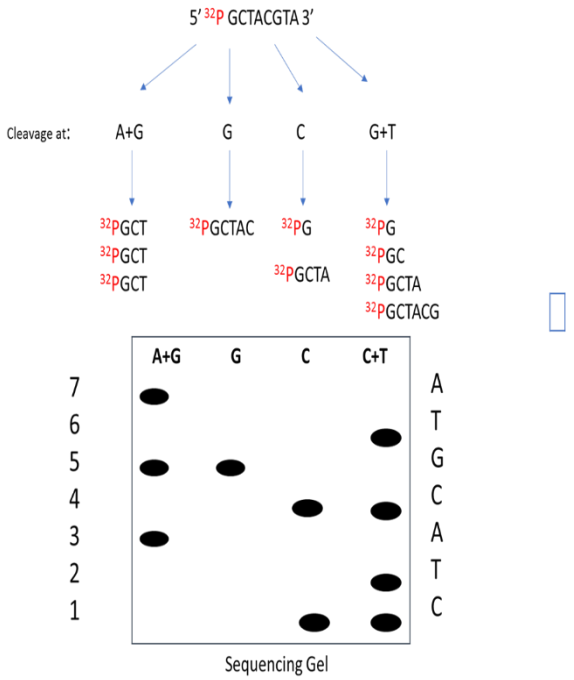

Fig. 1. Maxam–Gilbert sequencing method
Legend: The DNA fragment, marked at the 5' end with 32P is broken into different size nucleotides. The resulted fragments are ordered by size in an electrophoresis gel. Sequencing is obtained by autoradiography. Adapted from Maxam, A. M., & Gilbert, W. (1977) 74(2), 560–564 **[8]**

The Sanger method of sequencing

"... [A] knowledge of sequences could contribute much to our understanding of living matter."

Frederick Sanger

In 1977, Frederick Sanger developed a new technique for DNA sequencing based on the chain termination method. For this method, Sanger was awarded in 1980 with a second Nobel Prize in Chemistry **[9].** Also called "first generation sequencing", the technique means to synthesize the DNA chains on a template strand, but chain growth will stop when one of four possible dideoxy nucleotides, which lack a 3' hydroxyl group, will became incorporated, thereby preventing the addition of another nucleotide **[10].**

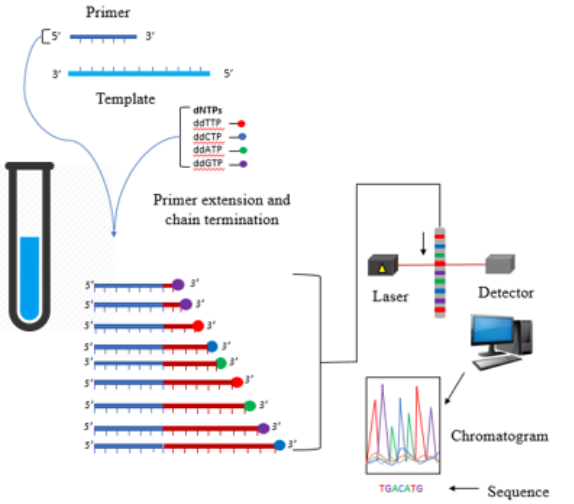

Fig.2. The enzymatic synthesis sequencing technique
Legend: In a tube, the DNA fragment to be sequenced is mixed with a primer, DNA polymerase, DNA nucleotides and the four dye-labeled chain-terminating dideoxy nucleotide. The mixture will be heated, cooled and then heated again, to denaturate the DNA and to help DNA polymerase to synthesize new DNA. At the end the tube will contain different lengths fragments. The ends of the fragments are labeled with dyes. Then the fragments are run through capillary gel electrophoresis. The detector records the fluorescence intensity and displays the result as a chromatogram. Adapted from Khan Academy **[10].**

The enzymatic synthesis technique. In a tube we combine the primer, DNA polymerase, DNA nucleotides (dATP, dTTP, dGTP and dCTP) with the DNA sample which is about to be sequenced. In the next step, the four dye-labeled, chain terminating dideoxy nucleotides are added. First, the template DNA needs to be denaturated, which means to separate each strands, so the mixture will be heated. After denaturation, the mixture will be cooled, so that the primer can bind to the single stranded template.

Once the primer has bound, the temperature is raised again, so that the DNA polymerase will synthesize new DNA, starting from the primer. DNA polymerase will continue

adding nucleotides to the chain until it adds a dideoxy nucleotide instead of a normal one. At this point, when a dideoxy nucleotide is added, no other nucleotides can be added, so this will be the last nucleotide from the given strand. This process is repeated in a number of cycles, and so in the end, different lengths fragments will be found in the tube. The ends of the fragments will be labeled with dyes.

The last step is to transfer the fragments to the capillary gel electrophoresis, where the short fragments will move quickly through the pores of the gel, while the long ones will move more slowly.

The detector records the data, which consists in a series of peaksin fluorescence intensity, and it is called 'a chromatogram'. The DNA sequence can be read from the chromatogram.

Later on the manually method was replaced by automated sequencing machines, in which the truncated DNA molecules were labeled with fluorescent tags and then were separated by size within thin glass capillaries and detected by laser excitation.

Sanger sequencing is used for relatively long stretches of DNA (up to about 900 base pairs). It is usually used to sequence individual pieces of DNA, such as bacterial plasmids or DNA copied in PCR, becoming a standard method in clinical genetics [**10].**

The automated Sanger method had dominated the industry for almost two decades and led to the only finished-grade human genome sequence.

Second-generation DNA sequencing

As the time passed by, for sequencing large numbers of human genomes, the Sanger method showed a need of technological improvement, despite its limitations **[11].**

In 2005 and the following years have marked the emergence of a new generation of sequencers, which were cheaper, more efficient and less time consumers. The new generation on sequencers can be divided by their working principle into: microelectrophoretic methods, sequencing by hybridization, real-time observation of single molecules and cyclic-array sequencing **[12].**

Within only a few days or hours, NGS technologies can sequence in parallel millions to billions of reads in a single run and the time required to generate the GigaBase sized reads. With fast development and wide applications, the next-generation sequencing is becoming better than the first generation such as Sanger sequencing [**13].**

The main characteristics of second generation sequencing technology are:

- generation of many millions of short reads in parallel
- speed up of sequencing the process compared to the first generation
- low cost of sequencing
- sequencing output is directly detected without the need for electrophoresis **[14].**

The first commercial next-generation DNA sequencing systems was launched by Roche's 454 technology in 2005, being able to produce sequences with very high throughput and at much lower cost than the previous technologies [14]. Today, the dominant second-generation sequencing platforms are HiSeq from Illumina and SOLiD from Life Technologies, as reported at AGBT **[15].**

Third-generation DNA sequencing

The third generations of sequencers is represented by Pacific Biosciences and Oxford Nanopore platforms. Pacific Biosciences uses fluorescent labelling (with different colors) as the previous technologies, and detects the signals in real time, as they are emitted every time the incorporation of the nucleotides occur. During the sequencing reaction, the DNA fragment is incorporated by the DNA polymerase with fluorescent labeled nucleotides. When a nucleotide is incorporated, it releases a luminous signal that is recorded by sensors. The detection of the labeled nucleotides is the equivalent of the determination of the DNA sequence **[14].**

The fundamental technology on which the third generation of sequencers is based on is SBS (sequencing by synthesis) by degradation, or direct physical inspection of the DNA molecule. It has a moderate current raw read accuracy, 1000 bp or longer current read length, moderate current throughput and a low cost per base. It takes only few hours from the beginning of sequencing until the primary result even if the data analysis is very complex due to the large data volumes **[2].**

The basic advantages of third- generation sequencing are: fast turn-around time, it requires minimal amounts of reagents/sample, no PCR amplification needed, more than 1000bp average read lengths **[16].**

FUNDAMENTALS OF NGS

Ten years ago next-generation sequencing (NGS) technologies appeared on the market, and since then, tremendous progress has been made.

All NGS platforms share a common feature, which is massively parallel sequencing of clonally amplified or single DNA molecules that are spatially separated in a flow gel **[17].**

An elementary step in each NGS workflow is a library construction. An NGS library is a collection of similar size DNA fragments and known adaptor sequences, added to the 5' and 3' ends of the DNA fragments. A library corresponds to a single sample and multiple libraries, each with their unique adaptor sequences. They can be sequenced in the same sequencing run. This technique of preparing the library is used in all types of NGS sequencing and involves four steps: DNA fragmentation or target selection, ligation of the adapters, size selection and library quantification and QC (quality control) **[18].**

The first step is DNA fragmentation, where the isolated double-strand DNA is fragmented in smaller pieces by

physical or enzymatic methods. These libraries are also called “fragment libraries”. If the sequence of a specific target is known, PCR amplification is used to produce DNA amplicons, which are called “amplicon libraries”.

The following step is to connect specific adaptors to the 5’ and 3’ end. These adaptors are between 20 to 40 bp fragments and they contain known sequences. There are two different types of adaptor. One adaptor sequence contains the primer annealing site for the sequencing primer, while the second type of adaptor is used to anchor the DNA fragment to a surface for sequencing (e.g. beads).

The next step is to select the library fragment sizes that we need for our sequencing. Generally there two size selection methods: gel electrophoresis and bead based size selection. In the gel electrophoresis method the adaptor library fragments are run in a gel to separate the fragments by size, and band corresponding the size of interest is collected. Using the bead based method, magnetic beads are used with buffer solution to isolate the fragment size of interest.

The last step is library quantification and QC. Accurate library quantification is important for successful template preparation. There are few library quantification commonly used. One of them is Bioanalyzer System; this method is measuring both library concentration and fragment size information. The second method is qPCR, and brings the most accurate library quantification information, as it measures only amplifiable library fragments but it doesn’t provide any information about the fragments size.

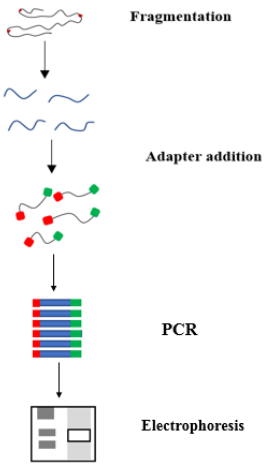

Fig.3. NGS library construction
Legend: The DNA fragment is broken into smaller fragments. Specific adaptors are connected to the 5’ and 3’ end. The library fragments with the adaptors will be run in a gel electrophoresis to arrange them by size and then run into Polymerase chain reaction (PCR). Adapted from Kchouk, M., Gibrat , J. F., & Elloumi, M. (2017) [13]

In contrary to Sanger sequencing, a NGS Sequencing can use the same protocol for all pathogens for both identification and typing applications **[19].**

There are no doubts that NGS brought a revolutionary progress to the scientific world, so that today we can use the sequencing methods for prenatal testing, cancer detection, transplant rejection, to detect pathogens and to determine cancer treatment.

In microbiology the NGS determines the DNA sequence of a complete bacterial genome in a single sequence run, and from these data, information on resistance and virulence. NGS sequencing allows whole genome sequencing (WGS), whole transcriptome shotgun sequencing (WTSS), RNA sequencing (RNA-seq), whole exome sequencing (WES), sequencing of targeted genes (TS) or candidate genes (CGS), active methylation and epigenetic markers **[5].**

Other clinical applications are: outbreak management, molecular case finding, characterization and surveillance of pathogens, rapid identification of bacteria, taxonomy, metagenomics approaches on clinical samples, and the determination of the transmission of zoonotic micro-organisms from animals to humans **[19].**

Improvements in technology have dramatically reduced the cost of DNA sequencing. According to National Human Genome Research Institute, the two following graphs show the cost of DNA sequence using Sanger-based chemistries and capillary-based instruments in 2001 and the cost of DNA sequence using 'second-generation' platforms from the beginning of 2008 **[20].**

In November 2008, the genomic company, Illumina announced that it can bring the price of genome sequencing below $100 in the next two years. It is expected that in few years the genome sequencing will be affordable to the majority of population, which can faster lead to the development of personalized medicine.

GlobalData analysts are predicting that genomics companies will become one day as big as the largest pharmaceutical companies and probably will dominate the pharmaceutical industry.

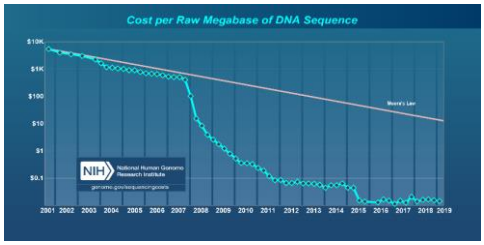

Fig.4. The evolution of sequencing cost
Legend: Sequencing cost per Mb 2001- 2019. Adapted from National Human Genome Research Institute [20]

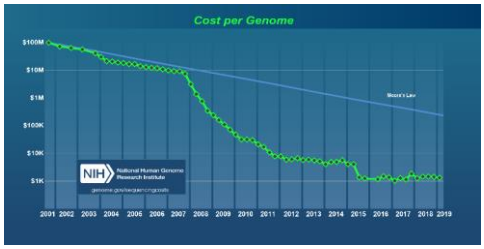

Fig.5. The evolution of sequencing cost.
Legend: Sequencing cost per genome 2001- 2019. Adapted from National Human Genome Research Institute [20]

At the moment there are many competing sequencing platforms on the market. According to "Labiotech" online science magazine: Illumina controls 75% of this market with its sequencing-by-synthesis (SBS) method. Its closest competitor is Thermo Fisher, which works on ion semiconductor sequencing (Ion Torrent), followed by Pacific Biosciences' single molecule real-time (SMRT) sequencing. Together, Thermo Fisher and Pacific Life Sciences control the remaining 25% of the market.

In April 2018, Genetic Engineering&Biotechnology News has developed a classification of top 10 sequencing companies:

10. Oxford Nanopore Technologies	5. Qiagen
9. 10x Genomics	4. Agilent Technologies
8. Genewiz	3. BGI Genomics
7. Pacific Biosciences of California (PacBio)	2. Thermo Fisher Scientific
6. Macrogen	1. Illumina

In the following parts, we will discuss about the most popular sequencing machines and the ones we work with in our laboratory.

Table I. Summary of NGS platforms and characteristics

Platform	Instrument	Reads per run	Avr Read length	Read type	Error type	Error rate (%)	Data generated per run (Gb)	Year
Illumina	MiniSeq	25M (maximum)	150	SE,PE	missmatch	1	7.5 (max)	2013
Illumina	MiSeq	25M (maximum)	300	SE,PE	missmatch	0.1	15 (max)	2011
Illumina	NextSeq	400M (maximum)	150	SE,PE	missmatch	1	120 (max)	2014
Illumina	HiSeq	5B(maximum)	150	SE,PE	missmatch	0.1	1.5 Tb (max)	2012
Illumina	HiSeq X	6B(maximum)	150	SE,PE	missmatch	0.1	1.8 Tb (max)	2014
Ion Torrent	PGM 314 chip v2	400.000-550.000	400	SE	indel	1	0.05 to 0.1	2011
Ion Torrent	PGM 315 chip v2	2-3 M	200	SE	indel	1	0.5 to 1	2011
Ion Torrent	PGM 315 Chip v2	4-5.5 M	400	SE	indel	1	1.2 to 2	2013
Ion Torrent	Ion Proton	60-80 M	200	SE	indel	1	10	2012
Ion Torrent	Ion S5 XL 520	3-5 M	400	SE	indel	1	1.2 to 2	2015
Ion Torrent	Ion S5 XL 530	15-20 M	400	SE	indel	1	0.3 to 0.5	2015
Ion Torrent	Ion S5 XL 540	16-80 M	400	SE	indel	1	NA	2015

Legend: Here we present the most popular sequencing platforms and their characteristics. Adapted from: Kchouk, M., Gibrat , J. F., & Elloumi, M. **[13]**

PGM and ION S5 SYSTEM

In 2011, Life technologies began commercializing and distributing the Ion Torrent Personal Genome Machine (PGM). Ion Torrent Personal Genome Machine or PGM is a sequencing platform that works on measuring pH rather than light to detect polymerisation events.

The PGM works on semi-conductor technology and ion-sensitive transistors to sequence DNA using only DNA polymerase and natural nucleotides, combining semiconductor sequencing technology with natural biochemistry. Ion Torrent semiconductor sequencing is using a similar technology to 454 pyrosequencing, but it is based on detection of the hydrogen ion released during the sequencing process, instead of using fluorescent labeled nucleotides like other second generation technologies.

The beginning of the sequencing is marked by the library preparation, which is commonly used for all NGS sequencers. After the library is ready, it is placed on a chip. The machine has a capacity of sequencing one chip per run. Every chip contains a set of micro wells, and each well has a bead with few identical fragments.

Every time a fragment incorporates a nucleotide in the pearl, a hydrogen ion is released which will change the pH of the solution. A sensor attached on the bottom of the micro well detects the change of pH, and converts it into a voltage signal. This voltage signal is proportional to the number of nucleotides incorporated.

This sequencing technology is able to read lengths which are longer and faster than other SGS sequencers, which represents its main advantage.

A major disadvantage of this sequencer is the dificulty of interpreting the homopolymer sequences, which will cause insertions and deletions (indel) **[14].**

The producer platform of PGM, Thermo Fisher, provides the following applications of the sequencer**:** DNA sequencing, epigenetic sequencing, fragment analysis, genotyping and genomic profiling, NGS, RNA sequencing [**21].** The Ion S5 systems are designed to enable a broad range of targeted next-generation sequencing (NGS) applications with speed and scalability.

The Ion S5 System, released in September, 2015 is using the speed of semiconductor sequencing with impressive on-board computing power. Easy to use with cartridge-based reagents, and high throughput sequencing applications. The Ion Chef System provides automated template preparation and reproducible chip loading for semiconductor sequencing machines **[22].**

A clinical study for deafness mutations has concluded that PGM is accurate for application to clinical diagnosis of common causative mutations and efficiently identified rare causative mutations and mutation candidates **[23].**

The main applications for PGM and Ion S5 are: microbial and metagenomic sequencing, targeted re-sequencing (gene panels) and clinical sequencing.

Table II. The main clinical applications for PGM and Ion S5 sequencing

Cancer research	Gene expression analysis	Microbiology/ Infectious disease research	Inherited disease research	Reproductive health research
- gene panels for SNPs - indels - copy number - gene expression - gene fusion analysis	- whole transcriptome RNA- Seq - targeted RNA sequencing - small RNA sequencing	- microbial whole genomes - microbial typing - metagenomics	- panels for targeted gene or whole exome analysis	- aneuploidy detection

ILLUMINA

Illumina is currently the leader in the NGS industry and most library preparation protocols are compatible with the Illumina system **[25].**

Illumina sequencing technology was based on sequencing by synthesis (SBS) technology, and it was founded in the Chemistry Department of Cambridge University in the mid 90's.

The new approach of sequencing was based on Cambridge scientists Shankar Balasubramanian, Ph.D. and David Klenerman, Ph.D. research. In their research, they were using fluorescently labeled nucleotides to observe the motion of a polymerase at the single molecule level as it synthesized DNA immobilized to a surface **[24].**

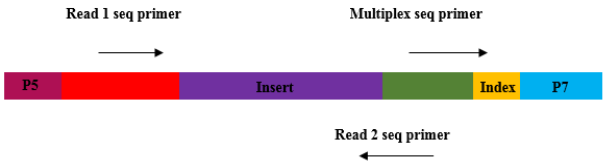

Fig.6. Architecture of a standard Illumina NGS library
Legend: The red and green spots are the adaptors. 'P5' and 'P7' are the sequences used for flow cell attachment and amplification. Adapted from Li, J., Batcha, A. M. N., Gaining, B., & Mansmann, U. R. (2015) [26]

Similar to the other methods, the DNA is first broken into fragments and run on a gel tray to separate them by size. From all the fragments, a 200-300 base pair fragment is selected for further replication through PCR.

An automated cluster generation is used to distribute the fragment library to the surface of a flow cell, amongst the adaptors. A process called bridge amplification occurs, creating copies of a specific molecule on the surface. As each new base is added, a camera records the location of each cluster by capturing the fluorescent signal. The sequence is actually the combination of these images. Even though is seems to be a slow process, each flow cell analyzes approximately 150 million of these clusters.

Table III. Illumina Benchtop Sequencers

	iSeq 100 System	MiniSeq System	MiSeq Series	NextSeq Series
Large whole genome sequencing (human, plant, animal)				X
Small whole genome sequencing (microbe, virus	X	X	X	X
Exome sequencing				X
Targeted gene sequencing (amplicon, gene panel)	X	X	X	X
Whole transcripom sequencing				X
Gene expression profiling with mRNA-seq				X
Targeted gene expression profiling	X	X	X	
Long-range amplicon sequencing	X	X	X	
miRNA and small RNA analysis	X	X	X	X
DNA-protein interaction analysis			X	X
Methilation sequencing				X
16s metagenomic sequencing		X	X	X

Legend: Applications of Illumina Benchtop Sequencers. Adapted from Illumina website [24]

Table IV. Illumina Large Scale Seqencers

	NextSeq Series	HiSeq 4000 System	HiSeq X Series	NovaSeq 6000 System
Large whole genome sequencing (human, plant, animal)	X	X	X	X
Small whole genome sequencing (virus, microbe)	X	X		X
Exome sequencing	X	X		X
Targeted gene sequencing (amplicon, gene panel)	X	X		X
Whole transcriptome sequencing	X	X		X
Gene expression profiling with mRNA Seq	X	X		X
miRNA and small RNA analysis	X	X		X
DNA protein interaction analysis	X	X		X
Methylation sequencing	X	X		X
Shotgun metagenomics	X	X		X

Legend: Applications of Illumina Large Scale Sequencers. Adapted from Illumina website [24]

Illumina also offers the highest throughput of all platforms and the lowest per-base cost. Read lengths of up to 300 bp are compatible with almost all types of application.

Unfortunately, the sample loading is technically challenging; because of the random scattering of clusters across the flow cells, the concentration of the library must be strictly controlled. When it's about 16S metagenomics, libraries must be diluted or mixed with a reference PhiX library to generate diversity **[25].**

CONCLUSION

The first method of sequencing came about half a century ago and it marked the beginning of a new era. The Sanger sequencing method lies at the heart of all other following methods. The evolution of sequencing has undeniable helped the scientific life to study biological systems at a higher level. Clinical laboratories have already started to use NGS as a diagnostic tool, while forensic research is still at the beginning.

NGS technologies are characterized by an impressive range of applications and high throughput, which gives us the opportunity to produce millions of reads in a short period of time and to use the obtained information in clinical and research use. We can conclude that since the first sequencing machine was released, many improvements have been made; starting with higher throughput, longer reads lengths, lower costs and lower error rate.

The technological advances in the field of genomics over the past quarter-century have led to substantial reductions in the cost of genome sequencing and it is predicted that in the following years will drop even more.

In this review, we presented a brief overview of the generations of sequencing technologies by beginning with the first-generation to the third generation. In the following years, many other sequencing platforms will appear, analyzing a larger amount of data (Terabyte) and leading us to a higher technological level, as the field of NGS development and applications is a fast-moving area of research

Acknowledgement: This work was supported by the grant "Chimeric Antigen Receptor Targeted Oncoimmunotherapy with Natural Killer Cells (CAR-NK)", POC 92/09/09/2016, ID: P_37_786, MySMIS code: 103662.

REFERENCES

1. Heather JM, Chain B. The sequence of sequencers: The history of sequencing DNA, 2016; 107(1): 1–8.
2. Lin Liu, Yinhu Li, Siliang Li, Ni Hu, Yimin He, Ray Pong, Danni Lin, Lihua Lu, and Maggie Law. Comparison of Next-Generation Sequencing Systems. Journal of Biomedicine and Biotechnology, 2012; ID 251364
3. Historic Figures (https://www.bbc.co.uk/history/historic_figures/watson_and_crick.shtml)
4. https://www.revolvy.com/page/Robert-W.-Holley
5. Mircea Covic. Medical Genetics, Third Edition, DNA sequencing, 2017: 138.
6. DNA sequencing by the Maxam-Gilbert chemical procedure. Laboratory Techniques in Biochemistry and Molecular Biology, 1983 (10): 230-285.
7. Peattie DA. Direct chemical method for sequencing RNA. *Proceedings of the National Academy of Sciences*, 1979; 76(4): 1760-1764.
8. Maxam AM, Gilbert W. A new method for sequencing DNA. *Proceedings of the National Academy of Sciences*, 1977; 74(2): 560-564.
9. https://www.nobelprize.org/prizes/chemistry/1980/sanger/biographical/
10. Khan Academy: DNA sequencing. https://www.khanacademy.org/science/high-school-biology/hs-molecular-genetics/hs-biotechnology/a/dna-sequencing

11. Metzker ML. Sequencing technologies-the next generation. Nature Reviews Genetics, 2009; 11(1): 31-46.
12. Shendure J, Ji H. Next-generation DNA sequencing. *Nature Biotechnology*, 2008; 26(10): 1135-45.
13. Kchouk M, Gibrat JF, Elloumi M. Generations of Sequencing Technologies: From First to Next Generation. *Biology and Medicine*, 2017; 9: 03.
14. Munroe DJ, Harris TJR. Third-generation sequencing fireworks at Marco Island. *Nature Biotechnology*, 2010; 28(5): 426-428.
15. Laura Moya Andérico. Ultrasequencing: Methods and Applications of the New Generation Sequencing Platforms, 2015.
16. Voelkerding KV, Dames SA, Durtschi JD. Next-Generation Sequencing: From Basic Research to Diagnostics. *Clinical Chemistry*, 2009; 55: 641-658.
17. Parson W, Strobl C, Huber G, Zimmermann B, Gomes SM, Souto L, Irwin J. Evaluation of next generation mtGenome sequencing using the Ion Torrent Personal Genome Machine (PGM). Forensic Science International: Genetics, 2013; 7(5): 543-549.
18. Deurenberg RH, Bathoorn E, Chlebowicz MA, Couto N, Ferdous M, García-Cobos S, et al. Application of next generation sequencing in clinical microbiology and infection prevention. *Journal of Biotechnology*, 2017; 243: 16-24.
19. National Human Genome Research Institute
20. https://www.thermofisher.com/order/catalog/product/4462921?SID=srch-srp-4462921
21. Wang L, Chen M, Wu B, Liu YC, Zhang GF, Jiang L, Ye J. Massively Parallel Sequencing of Forensic STRs Using the Ion Chef™ and the Ion S5™ XL Systems. *Journal of Forensic Sciences*, 2018.
22. Nishio SY, Hayashi Y, Watanabe M, Usami SI. Clinical Application of a Custom AmpliSeq Library and Ion Torrent PGM Sequencing to Comprehensive Mutation Screening for Deafness Genes. *Genetic Testing and Molecular Biomarkers*, 2015; 19(4); 209–217.
23. https://emea.illumina.com/science/technology/next-generation-sequencing/illumina-sequencing-history.html?langsel=/ro/
24. Van Dijk EL, Auger H, Jaszczyszyn Y, Thermes C. Ten years of next-generation sequencing technology. *Trends in Genetics*, 2014; 30(9): 418-426.
25. Li J, Batcha AMN, Gaining B, Mansmann UR. An NGS Workflow Blueprint for DNA Sequencing Data and Its Application in Individualized Molecular Oncology. Cancer Informatics

APLICAȚII MODERNE ALE SECVENȚIERII DE NOUĂ GENERAȚIE (NGS)

REZUMAT

Secvențierea ADN se referă la determinarea ordinii corecte a bazelor de nucleotide dintr-o macromoleculă de ADN folosind tehnologii de secvențiere. Prima metodă de secvențiere bazată pe sinteza enzimatică sau metoda Sanger a deschis calea revoluției în domeniul genomicii și a altor domenii științifice.

În ultimii zece ani, au fost lansate platforme de secvențiere ale ADNului care pot analiza un volum uriaş de informaţii într-un timp mult mai scurt. Apariția ultimelor generații de secvențe a schimbat viziunea analizei și a înțelegerii corpurilor vii. Progresul a accelerat cercetarea biologică și biomedicală prin reunirea secvențializării ADN-ului, secvențierii epigenetice, analizei fragmentelor, genotipării și profilării genomice. Capacitatea aparatelor de a citi lungi secvenţe de nucleotide, timpul mai scurt până la rezultatul analizei și un cost total mai mic al secvențierii ADN-ului, au făcut ca acesta să fie accesibil pe scară largă și mult mai eficient.

În aceast review, prezentăm o scurtă evoluție a metodelor de secvențiere de la început până la zilele noastre și gama de aplicații de bază pentru tehnologiile NGS.

Cuvinte cheie: ADN, secvenţiere, metoda Sanger, molecule, nucleotide

MODIFIED LANGENDORFF DEVICE FOR RAT HEART DECELLULARIZATION

DANIEL BONCIOG[1], LILIANA MÂȚIU-IOVAN[1], GRETA BĂRBULESCU[3], CAIUS BURIAN[2], DANIEL GOJE[3], PAUL BUICĂ[2], VIRGIL PĂUNESCU[2,3], VALENTIN ORDODI[1,2]

[1]Politehnica University of Timișoara, 2 Victoriei Square, RO-300006, Timișoara, România
[2]OncoGen Research Center, Pius Bânzeu Clinical Emergency Hospital, 156 Liviu Rebreanu Bv, RO-300723, Timișoara, România.
[3]University of Medicine and Pharmacy "V. Babeș" Timișoara, 2 Eftimie Murgu Square RO-300041, Timișoara, România

ABSTRACT
In this paper we propose the design and implementation of a modified Langendorff experimental device, pressure controlled, used to decellularize the heart with a sodium dodecyl sulfate (SDS) surfactant solution to obtain cardiac biomatrix. The experimental device consists of two constructive parts: a hydraulic part that provides through a peristaltic pump and a pressure transducer, infusion retrograde through the aorta of the heart under constant pressure regime, as well as an electronic part that constitutes the regulator of the experimental device. The decellularization solution is recirculated during the physico-chemical process, so that by serial spectrophotometric determinations of the concentration of deoxyribonucleic acid (DNA) and proteins in this solution, the kinetics of the decellularization and can be determined, respectively, when it is completed.
Keywords: Langendorff, electronic pressure regulator, decellularization, cardiac biomatrix.

INTRODUCTION

In recent years we have witnessed a major development of the medical sciences, with a significant impact on the increase of life expectancy. Thus, modern medicine has to solve more and more cases with degenerative pathology of tissues and organs which demands finding viable possibilities for their replacement [1,2,3]. Modern transplantology involves two major problems: (i) the number of potential organ and tissue donors is significantly lower compared to the number of patients in need of such treatment, which leads to the formation of long waiting lists and (ii) the issue of immune mediated rejection involving treatments aggressive so as not to compromise the respective graft. To these problems are added those of a moral and religious aspects that further limit the possibility of performing a transplant operation. Due to these aspects, tissue engineering is looking for viable solutions for obtaining in vitro functional tissues and organs that can be transplanted. One of the goals of bioengineering is the obtaining of biomaterials that allow the growth and differentiation of some cell types, thus being able to fulfill a basic requirement for the realization of a three-dimensional cellular construct suitable for implantation in a human body [4,5]. The decellularization of an organ as a whole offers the best three-dimensional biomaterial suitable for recellularization with the recipient's own stem cells and thus obtaining a functional and self-organ. In the case of the heart, to obtain a biomaterial with adequate three-dimensional structure, several protocols were applied on both large animals and small animals. Ott applied coronary anterograde perfusion to the rat heart using three surfactants for decellularization: sodium dodecyl sulfate (SDS), polyethylene glycol (PEG) and Triton X-100, respectively enzyme-based methods: trypsin in the presence of EDTA-Na_2 and deoxycholic acid. The authors observed that protocols that used SDS as a decellularizing agent are superior to those that used PEG, Triton X-100 or enzymes [6,7]. Anterograde coronary perfusion with SDS for 12 hours allowed to obtain a fully decellularized good quality biomaterial. Most experimental devices used to decellularize the various organs are based on the retrograde perfusion principle described by Langendorff using the arterial system of the respective organ. The purpose of this paper consisted

Received September 15th 2019. Accepted November 20th 2019. Address for correspondence: Valentin Ordodi, PhD, Politehnica University of Timișoara, 2 Victoriei Square, RO-300006, Timișoara, România; phone: +40-256-404219; e-mail: vali.medtm99@gmail.com

in the design and implementation of a pressure controlled Langendorff type device for decellularizing the rat heart [8,9,10].

EXPERIMENTAL DEVICE

The experimental device respects the principle described by Langendorff and from functional point of view it is a pressure controlled device. It maintains constant coronary perfusion pressure by varying the minut-volume rate of decellularization solution that enters in the aorta [11,12,13]. In figure 1.A. we observe the experimental device as a whole, and in figure 1.B. its block diagram.

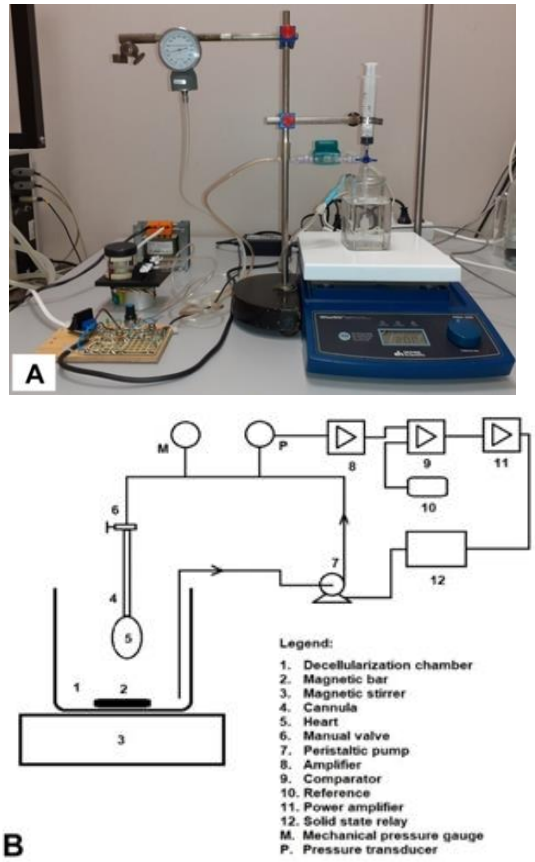

Fig. 1. A. Experimental device. **B.** Block diagram

The heart (Fig. 1B.5) prepared for decellularization is fixed to the tip of a special cannula (AD Instruments) (Fig. 1B.4) and inserted into a decellularization chamber (Fig. 1B.1) made of plastic material with the volume of 100 cubic centimeters. It contains the decellularization solution: SDS 1% homogenized during the experiments by means of a magnetic stirrer (Fig. 1B.2 and 1B.3). Thus the composition of the solution is constant at any point of the chamber at the one time, thus allowing the collection of samples for biochemical determinations. The decellularization solution is aspirated from decellularization chamber by the peristaltic pump (Fig. 1B.7) and reintroduced into the heart via of the cannula. The manual valve (Fig. 1B.6) with which the cannula is provided, is used for the initial filling of the hydraulic circuit of the experimental device and the elimination of any air bubbles. The perfusion pressure of the heart is the pressure on the discharge branch of the peristaltic pump and is permanently monitored by the pressure resistive transducer (Fig. 1B.P). Additionally, it is read by the researcher on the mechanical manometer (Fig 1B.M). The operation of the peristaltic pump is controlled by the automation system that brings together the following modules: pressure amplifier (Fig. 1B.8) that processes the signal generated by the resistive pressure transducer; the comparator module (Fig. 1B.9), which receives both the amplified signal from the pressure transducer and a reference voltage regulated by the researcher from potentiometer (Fig. 1B.10). Its scale is directly graded in mmHg. The output of this module reaches a power amplifier (Fig. 1B.11) and via a solid state relay (Fig. 1B.12) controls the peristaltic pump function.

EXPERIMENTAL PROTOCOL

Testing and validation of the experimental device was performed by decellularizing five Sprague Dawley rat rats weighing between 350 and 400 g. The harvesting of hearts was done in compliance with international law (The Guide for the Care and Use of Laboratory Animals published by the National Institute of Health no.85-23) and the recommendations of the Ethics Commission of UMF „V Babeș" Timișoara. In all cases, VIMA general anesthesia with sevoflurane was used. induction was performed with sevoflurane 8% in oxygen in a special chamber, and maintenance was performed with sevoflurane 3.5% through a facial mask for rats until the heart was excised. In the first step, the abdominal cavity is opened and the heparin sodium is injected into the inferior vena cava 100 IU / Kg. After 4-5 minutes, the thoracic cavity is opened by cutting the ribs and the heart is rapidly excised with a fragment as long as the aorta. It is inserted into a Petri dish with a cold solution of heparinized physiological sodium chloride and the dissection is continued until the cord and a fragment of aorta about 1 cm long are prefectly isolated [14,15]. The heart thus processed is fixed with a silk surgical thread on the cannula of the Langendorff type device and infused for 600 minutes with a 1.5% SDS solution [16]. The solution volume in the device was 120 cm^3. At 30 min intervals, 30 uL samples were taken to determine the concentration of nucleic acids and proteins in the decellularization solution. These determinations were performed using the ultraviolet spectrophotometric method. The proteins have a maximum absorption at 280 nm at neutral pH. Nucleic acids under the same conditions have a maximum absorption at 260 nm, so that the two analytes can be determined simultaneously

without their separation [17,18,19]. A NanoDrop ND-1000 computerized microspectrophotometer was used. The device performs the measurements directly, without the need for other reagents, and the results are displayed in ng/µL for nucleic acids and in mg/mL for proteins.

RESULTS AND DISCUSSIONS

Following the processing of the experimental data, the final moment of decellularization could be established, considered as the time when the concentration of the two determined analytes became constant. Figure 2 shows graphically the average values of deoxyribonucleic acid and protein concentration respectively for the five experiments performed.

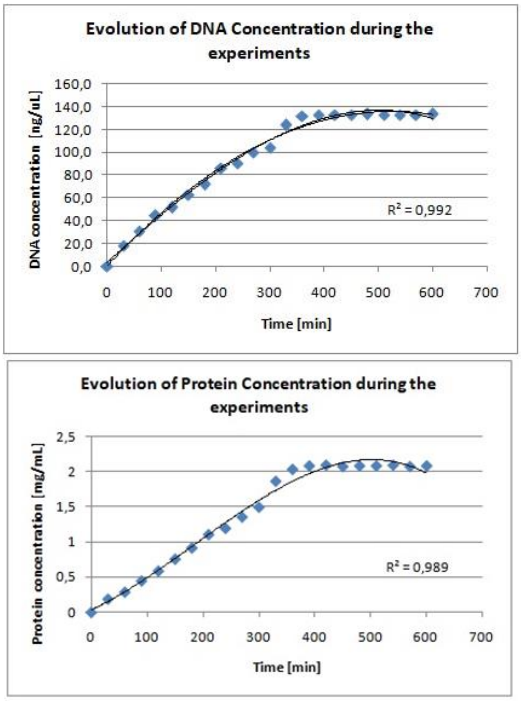

Fig. 2. Evolution of DNA and protein concentration during the heart decellularization (median values).

The increase of the concentration of the two analytes is described very well by the following polynomial equations of order 3 (Correlation coefficient, $R^2 > 0.95$ in both cases). We can say that these equations apply to any experiment of decellularization of the rat heart under the conditions presented.

$$C_{DNA}\ [ng/\mu L] = -4 \cdot 10^{-0,7} \cdot t^3 + -0,000 \cdot t^2 + 0,439 \cdot t + 3,007$$

$$C_{Protein}\ [mg/mL] = -2 \cdot 10^{-0,8} \cdot t^3 + 10^{-0,5} \cdot t^2\ 0,003 \cdot t + 0,024$$

From the analysis of the experimental data it is observed that at the minute 400 the decellularization can be considered completed because the concentration of both analytes reaches a stable maximum.

CONCLUSIONS

The proposed experimental device and the method presented are well suited for the decellularization of the rat heart in order to obtain biomaterials that can then be repopulated with autologous cardiac muscle cells obtained by in vitro differentiation of mesenchymal stem cells.

REFERENCES

1. Peter MC, Thomas WG, Stephen FB. An overview of tissue and whole organ decellularization processes. *Biomaterials*, 2011; 32: 3233-3243.
2. Hawkins JA, Hillman ND, Lambert LM, et al. Immunogenicity of decellularized cryopreserved allografts in pediatric cardiac surgery: comparison with standard cryopreserved allografts. *J Thorac Cardiovasc Surg*, 2003; 126: 247-52.
3. http://www.crestinortodox.ro/sanatate-si-stiinta/72679-moartea-cerebrala.
4. Murray JE. Organ transplantation: the practical possibilities. Boston ed., 1966; 54-67.
5. Gilbert TW, Sellaro TL, Badylak SF. Decellularization of tissues and organs. *Biomaterials*, 2006; 27: 3675-83.
6. Ott HC, Matthiesen TS, Goh SK, Black LD, Kren SM, Netoff TI, Taylor DA. Perfusion decellularized matrix: using nature's platform to engineer a bioartificial heart. *Nat Med*, 2008; 14(2): 213-21.
7. Nakayama KH, Batchelder CA, Lee CI, Tarantal AF. Decellularized rhesus monkey kidney as a three-dimensional scaffold for renal tissue engineering. *Tissue Eng Part A* 2010;16(7): 2207-16.
8. Weymann A, Loganathan S, Takahashi H, Schies C, Claus B, Hirschberg K, et al. Development and evaluation of a perfusion decellularization porcine heart model-generation of 3-dimensional myocardial neoscaffolds. *Circulation journal: official journal of the Japanese Circulation Society* 2011; 75(4): 852-860.
9. Weymann A, Radovits T, Schmack B, Li S, Korkmaz S, Soós P, et al. In vitro generation of atrioventricular heart valve neoscaffolds. *Artificial organs* 2014; 38(7): E118-E128.
10. Badylak SF, Weiss DJ, Caplan A, Macchiarini P. Engineered whole organs and complex tissues. *Lancet*, 2012; 379**:** 943.
11. Perju D, Suta M, Todincă T, Rusnac C. Echipamente de automatizare pneumatice de joasa presiune. Aplicaţii. Pneumatica Collection, Politehnica Timisoara Ed., 2001.
12. Perju D, Suta M, Rusnac C, Brusturean GA. Automatizarea proceselor chimice. Aplicaţii. Pneumatica Collection, Politehnica Timisoara Ed., 2005

13. Ionescu G et al. Traductoare pentru automatizări industriale. Vol I. Ciclul manualului inginerului automatist. Tehnica Bucharest Ed., 1985.
14. Blasig IE, Ebert B, Hennig C, Pali T, Tosaki A. Inverse relationship between ESR spin-trapping of oxy-radicals and degree of functional recovery during myocardial reperfusion in isolated working rat heart. *Cardiovasc Res* 1990; 24: 263-270.
15. Chen Z, Li T, Zhang B. Morphine postconditioning protects against reperfusion injury in the isolated rat hearts. *J Surg Res* 2008; 145: 287-294.
16. Mirica N, Luculescu M, Răducan A, Ordodi V, Duicu O, Borya C, Fira–Mlădinescu O, Muntean D. Dichotomic effects of Diayoxide and Cyclosporine A on contractile function and infarct size in Langendorff perfused rat hearts. Proceedings of 8th International Congress on Coronary Artery Disease, Oct 11-14 , 2009, Prague Czech Republic, Ed. Medimond international Proceedings, 21-26.
17. Manta I, Cucuianu M, Benga G, Hodârnău A. Metode biochimice în laboratorul clinic. Ed. Dacia, Cluj-Napoca, 1976.
18. www.promega.ro/resources
19. www.nanodrop.com.

DISPOZITIV LANGENDORFF MODIFICAT PENTRU DECELULARIZAREA INIMII DE ȘOBOLAN

REZUMAT

În lucrarea de față ne propunem proiectarea și realizarea unui dispozitiv experimental de tip Langendorff, controlat in presiune, folosit pentru decelularizarea cordului cu o soluție tensioactivă de sodiu dodecil sulfat (SDS) în vederea obținerii biomatricilor cardiace. Dispozitivul experimental este format din două părți constructive: o parte hidraulică care asigură prin intermediul unei pompe peristaltice și a unui traductor de presiune, perfuzia retrogradă prin aorta a cordului în regim presional constant, precum și o parte electronică care constituie regulatorul dispozitivului experimental. Soluția de decelularizare se recirculă pe parcursul procesului fizico-chimic, astfel încât prin determinări spectrofotometrice seriate a concentrației de acid dezoxiribonucleic (ADN) și proteine din această soluție se poate determina cinetica decelularizării respectiv momentul în care acesta este finalizată.

Cuvinte cheie: Langendorff, reglator electronic de presiune, decelularizare, biomatrice cardiacă

B*08:01 HLA CLASS I AND CLASS II ALLELES AND HAPLOTYPES FREQUENCIES PATIENTS WITH HEMATOLOGICAL DISEASES IN THE WESTERN PART OF ROMANIA

ELENA GAI[1], DIANA LUNGEANU[2], SMARANDA ARGHIRESCU[3], CRENGUTA LIVIA CALMA[1,4], VIRGIL PAUNESCU[1,4]

[1]OncoGen - Centre for Gene and Cellular Therapies in Cancer, Emergency Clinical County Hospital "Pius Brînzeu" Timișoara
[2]Centre for Modelling Biological Systems and Data Analysis, Department of Functional Sciences, "Victor Babeș" University of Medicine and Pharmacy, Timișoara, Romania
[3]Departement of Transplant, Emergency Clinical Hospital "Louis Ţurcanu",
[4]Department of Functional Sciences, "Victor Babeș" University of Medicine and Pharmacy, Timișoara, Romania

ABSTRACT
The present study was conducted between 2015 and 2018 and it aimed to investigate the haplotypes incidence in acute lymphoblastic leukemia (ALL), acute myeloid leukemia (AML) and aplastic anemia (AA) in Western Part of Romania. Sequencing-based typing (SBT) technique using SeCore ONE LAMBDA kits was used to type HLA genes class I and II. The frequencies of the alleles for the hematologic disease were calculated and compared.
Keywords: HLA genes class I and II, haplotypes, acute lymphoblastic leukemia (ALL), acute myeloid leukemia (AML), aplastic anemia (AA), sequencing-based typing (SBT) technique

INTRODUCTION

The major histocompatibility complex (MHC) plays a fundamental role in immune response [1][2] and it's first mentioned involvement in human affections was highlighted in leukemia [3].

In humans, the major histocompatibility complex is localized on chromosome 6 being expanded on about 4 centiMorgan (cM) of DNA (4 × 106 pairs of bases) and comprising approximately 200 genes [4].

HLA (Human leukocyte antigen) represents the human version of MHC and encodes proteins on the surface of antigen-presenting cells (APC) [5]. The HLA A, B, and C genes correspond to the class I MHC exhibit intracellular peptides, HLA DP, DM, DQA, DQB, and DR genes correspond to the class II MHC exhibit extracellular peptides while the HLA genes corresponding to MHC class III coding part of the complement components system. Of these, there are three genes containing α chains and are called class I (HLA-A, -B, and-C) and three pairs of genes containing α and β chains and are called class II (HLA-DR,-DP, and-DQ) [6] [7].

Acute leukemia comprises a group of oncohaematological diseases with multifactorial origins. The results of an epidemiological [8] study show that acute lymphoblastic leukemia (ALL) occurs mainly in children, while acute myeloblastic leukemia (AML) is observed in young people, and its incidence increases with age [9].

Aplastic anemia (AA) is a rare condition that threatening the existence of hematopoietic stem cells, anemia characterized by peripheral blood cytopenia and hypoplasia of the bone marrow. This occurs by destroying hematopoiesis by cytotoxic T cells. Certain human leukocyte antigen (HLA) alleles play a role in activating clones with autoreactive T lymphocytes in patients with AA [10].

The purpose of this study is to investigate the incidence of haplotypes in patients with ALL, AML and AA.

Received July 10th 2019. Accepted October 12th 2019. Address for correspondence: Elena Gai, Biol. PhD, OncoGen - Centre for Gene and Cellular Therapies in Cancer, Emergency Clinical County Hospital "Pius Brînzeu" Timișoara, Liviu Rebreanu Bvd. 156, RO-300723, Timisoara, Romania; phone: +40356433282, +40374161282; e-mail: elagai@yahoo.com

MATERIALS AND METHODS

Patients

HLA typing has been performed in the HLA department of OncoGen - Centre for Gene and Cellular Therapies in Cancer, Emergency Clinical County Hospital "Pius Brînzeu" Timișoara, who has accreditation from the National Transplant Agency to perform HLA-print.

In the current study, we included 554 records from which 264 were receptors. We identified 194 patients with one of the three disorders analyzed (ALL, AML, and AA) who underwent bone marrow transplantation. Of the 194 cases, 82 were diagnosed with acute lymphoid leukemia, 67 with acute myelogenous leukemia and 45 with aplastic anemia.

Method

The studied samples were collected from 554 children patient's of Emergency Clinical Hospital "Louis Ţurcanu", Departement of Transplant, between 2015 and 2018. According to the norms of international and national ethics, informed consent has been obtained from all the subjects or their legal guardians regarding the use of data in this study [11].

Collection, transport, and storage of specimens were carried out in accordance with applicable regulatory requirements. The whole blood samples were collected in vacutainer tubes with 2 mL (3.6 mg) K3-EDTA ethylendiaminotertraacetic from patients diagnosed with LAL, LAM, and AA.

Extraction

The MagNA Pure LC automatic extraction was performed using 2 mL of whole blood samples and the MagnaPure LC Automatic DNA Extraction kit containing the wash buffer I, wash buffer II, lysis buffer, proteinase K and magnetic glass particles suspension (MGPs). The extraction kit and the instrument use magnetic ball technology to purify genomic DNA from the bloodstream. Magnetic particles are used to capture DNA in the solution. The DNA on the magnetic particles is washed and then it is eluted from the magnetic particles in the solution for use.

The MagnaPure system required a 120-minute time for the 100 µl protocol to complete the DNA isolation from 32 samples.

The verification of the DNA concentration extracted from each sample was carried out with the Qubit 3.0 Fluorometer.

HLA genotyping

HLA Genotyping was carried out using the sequencing-based typing (SBT) method, using SeCore ONE LAMBDA kits to determine the class I and class II HLA allele.

Pre-amplification for class I was performed with a specific Amplification Mix class I (A, B, C) and FastStart Taq using for each sample 20 mL mixture and 5 mL DNA. Pre-amplification for class II was performed with a special class II Amplification Mix (DQB1 and DRB1) and FastStart Taq using each case of 23 mL mixture and 2 mL DNA.

The samples thus prepared were introduced in ThermoCycler GeneAmp Applied Biosystems 9700 program SECORE PRE where the amplification was carried out comprising several stages and cycles during the duration of 60 minutes. The amplification product has been checked by an agarose gel migration 2%. It then followed the purification phase with EXO-SAP for the elimination of unincorporated dNTP stage that was performed using ThermoCycler GeneAmp Applied Biosystems 9700 program SECORE EXOSAP consisting of a cycle of 20 minutes at 37 °C and a 20-minute cycle at 80°C.

Post-amplification was performed using the specific kits of each class I and class II and the corresponding amplicons. The samples thus prepared were introduced in the GeneAmp thermocycler Applied Biosystems 9700 program SECORE POST for the actual amplification.

The sequencing fragments were then purified by precipitation with ethanol and skated using Hi-Di formamide and PPT buffer. The denatured product has been detected by the electrophoresis on 16 capers using the genetic Analyzer of automatic sequencing genetically analyzer ABI 3130xL.

The obtained electropherograms were interpreted with the HLA SBT uTYPE 7.0 program to process the data files of DNA samples. Data files are generated from the samples processed with SeCore sequencing kits and the Aplied Genosystem Genetic Analyzer. Analysis and identification of HLA genes was done by comparison with the IPD (Immuno Polymorphism Database) database-IMGT (International ImMunoGeneTics)/HLA [12] [13].

Data analysis

Univariate descriptive statistics included the observed frequency counts (percentage). To investigate the statistical significance of observed differences in allele frequences within the analyzed groups, a Chi-square test [14] [15] or the Fisher-exact test [16] were applied.

Furthermore, inter-haplotype correlation and exploratory principal component analysis (PCA) was conducted to investigate the underlying associations of haplotypes in the three blood disorders. Kaiser-Meyer-Olkin (KMO) test of sampling adequacy and Bartlett's test of sphericity were applied to verify the data suitability for factor analysis. The scree plots and the eigenvalues over 1 were considered as criteria for deciding the appropriate number of factors to be extracted. The resulting factors were used to explore the possible underlying haplotype structure in the blood conditions within the analyzed database.

The descriptive statistics (i.e. the frequency tables of observed alleles) include both four-digit HLA-typing (i.e. high-resolution profiles with first two nomenclature fields) and two-digit HLA-typing. The decision to neither drop the

two-digit records nor reduce all the records to two-digit resolution was based on the consideration of the informative character of these valuable data existing in this historical database.

All reported probability values were two-tailed and a 0.05 level of significance was considered, while marking the highly significant values, as well. Data analysis was conducted with the statistical software IBM SPSS v.20 and the R v.3.4.1 software packages.

RESULTS AND DISCUSSION

We identified 194 patients with one of the three disorders analyzed (ALL, AML, or AA) who underwent bone marrow transplantation. Of the 194 cases, 82 (31.1%) was diagnosed with acute lymphoid leukemia, 67 (25.4%).with acute myelogenous leukemia and 45 (17.0%) with aplastic anemia. Table I shows the observed blood disorders in the study population, with their respective frequencies and number of homozygous cases.

Table I. The observed types of blood disorder in the study population

Blood disorder	Observed count frequency (%)	HLA-A homozygotes	HLA-B homozygotes	HLA-C homozygotes	HLA-DRB1 homozygotes	HLA-DQB1 homozygotes
Acute lymphoblastic leukemia (ALL)	82 (31.1%)	14	6	6	6	12
Acute myeloid leukemia (AML)	67 (25.4%)	7	8	8	10	16
Aplastic anemia (AA)	45 (17.0%)	5	2	2	7	8
Immunodeficiency	8 (3.0%)	–	–	–	–	
Myelodysplastic syndrome	8 (3.0%)	–	–	–	1	1
Wiskott–Aldrich syndrome	6 (2.3%)	–	–	1	–	–
Hodgkin's lymphoma	5 (1.9%)	3	–	1	–	1
Chronic granulomatous disease	4 (1.5%)	1	1	1	–	–
Neutropenia	4 (1.5%)	–	–	–	–	–
Lymphoblastic lymphoma	3 (1.1%)	1	–	–	–	1
Non-Hodgkin lymphoma	3 (1.1%)	–	–	–	–	–
Medullary aplasia	2 (0.8%)	1	–	–	–	–
Paroxysmal nocturnal hemoglobinuria	2 (0.8%)	–	–	–	1	1
Lymphoma	2 (0.8%)	1	–	–	–	–
Myelofibrosis with myeloid metaplasia (MMM)	2 (0.8%)	–	–	–	–	–
Severe combined immunodeficiency (SCID)	2 (0.8%)	1	–	1	–	–
Purine nucleoside phosphorylase deficiency	1 (0.4%)	–	–	–	–	–
Langerhans cell histiocytosis	1 (0.4%)	–	–	–	–	–
Juvenile myelomonocytic leukemia (JMML)	1 (0.4%)	–	–	–	–	–
Myelomonocytic leukaemia	1 (0.4%)	–	–	–	–	–
Multiple myeloma	1 (0.4%)	–	–	–	–	1
Lymphohistiocytosis	1 (0.4%)	1	–	1	–	–
Anaplastic large cell lymphoma	1 (0.4%)	1	–	–	–	–

Chronic lymphocytic leukemia	1 (0.4%)	–	–	–	–	–
Chronic myelogenous leukemia (CML)	1 (0.4%)	–	–	–	–	–
Chronic myelogenous leukemia in the lymphoid blastic phase	1 (0.4%)	–	–	–	–	–
Pancytopenia	1 (0.4%)	1	–	–	–	–
Idiopathic thrombocytopenic purpura	1 (0.4%)	–	–	–	–	–
Refractory thrombotic thrombocytopenic purpura	1 (0.4%)	–	–	1	–	–
Myeloid sarcoma	1 (0.4%)	–	–	–	–	–
Shwachman-Diamond syndrome	1 (0.4%)	–	–	–	–	–
Griscelli syndrome	1 (0.4%)	–	–	–	–	–
Nijmegen breakage syndrome	1 (0.4%)	–	–	–	–	–
Thalassemia	1 (0.4%)	–	–	–	–	–
Thrombocytopenia	1 (0.4%)	–	–	–	–	1
Total	**264 (100%)**					

Tables II (a, b, c, d, e) present the synthesis with the allele groups identified within the three groups of disorders analyzed ALL, AML, and AA. Each HLA type was counted once for a case (i.e. the allele was counted once for the homozygous cases).

One limitation of the present study is the resolution discrepancy for the HLA-typing in the database, though we chose to keep the two-digit resolution data for their informative value in future studies. Another caveat is generated by the limited number of cases in the database and subsequent relatively low frequency of observed alleles and haplotypes, nevertheless bringing valuable information for future studies on HLA patterns in blood conditions.

The frequency of the human leucocyte antigen (HLA)-A*24:02 allele (22.0%), HLA-A*03:01 (20.7%) and HLA-A*32:01 (18.3%) were significantly higher in patients with ALL compared with AML and AA. Among patients with AML, the frequency of the HLA-A11:01 allele (11.9%) was significantly higher, whereas the frequency of the HLA-A*02:01 allele (46.7%) was also significantly higher in patients with AA and ALL- HLA-A*02:01 allele (42.7%).
This study indicated that the frequency of the HLA-B*08:01 allele (15.6%) and the HLA-B*14:02 (13.3%) allele may play a predisposing role in patients with AA. The frequency of the HLA-B*18:01 (13.3% and HLA-B* 35:01 (13.4%) alleles may be associated with high risk of AML vs. HLA-B* 44:02 (12.2%) and HLA-B* 51:01 (15.9%) with high risk of ALL, respectively.

Significant positive association with the AA disease was found for HLA-C* 07:01 (37.8%) and HLA-C* 06:02 (17.8%) vs. HLA-C* 12:03 (20.9%). and HLA-C* 08:02 (11.9%) association with AML and HLA-C* 04:01 (24.4%) and HLA-B* 15:02 (9.8%)association with ALL.

HLA-DRB1* 01:01, HLA-DRB1* 03:01 and HLA-DRB1* 13:01 were the most frequent alleles in the patients with AA (17,8%). HLA-DRB1* 07:01 (20.9%) and HLA-DRB1 *11:01 (14.9%) alleles were detected in AML patients. HLA-DRB1* 11:04 (25.6%) and HLA-DRB1 16:01 (17.1%) were the most frequent alleles in the ALL patients.

Three alleles including HLA-DQB1 03:01 (45.1%), HLA-DQB1 05:02 (23.2%) and HLA-DQB1 05:01 (19.5%) were significantly frequent in ALL patients. HLA-DQB1 02:01 (22.2%), HLA-DQB1 03:02 (20.0%) and HLA-DQB1 06:03 (20%) alleles were observed in AA and HLA-DQB1 02:02, significantly less frequent, was present in patients with AML (17.9%).

Table II a. The frequencies of HLA-A* allele identified within ALL, AML, and AA.

HLA-A* allele	Total[(a)(b)] (n=194)	ALL [(a)(c)] (n=82)	AML [(a)(d)] (n=67)	AA[(a)(e)] (n=45)	p-value [(f)]
–	2 (1.0%)	1 (1.2%)	–	1 (2.2%)	–
01:XX	7 (3.6%)	3 (3.7%)	3 (4.5%)	1 (2.2%)	0.89
01:01	43 (22.2%)	17 (20.7%)	14 20.9%)	12 (26.7%)	0.71
02:XX	10 (5.2%)	3 (3.7%)	5 (7.5%)	2 (4.4%)	0.60
02:01	82 (42.3%)	35 (42.7%)	26 (38.8%)	21 (46.7%)	0.71
02:05	2 (1.0%)		1 (1.5%)	1 (2.2%)	–
02:07	2 (1.0%)	1 (1.2%)		1 (2.2%)	–
02:11	4 (2.0%)	2 (2.4%)			–
02:17	2(1.0%)	1 (1.2%)		1 (2.2%)	–
03:XX	4 (2.0%)	1 (1.2%)	1 (1.5%)	2 (4.4%)	0.45
03:01	28 (14.4%)	17 (20.7%)	8 (11.9%)	3 (6.7%)	0.075
03:02	3 (1.5%)	1 (1.2%)	2 (3.0%)		–
11:XX	1 (0.5)		1 (1.5%)		–
11:01	28 (14.4%)	9 (11.0%)	12 (17.9%)	7 (15.6%)	0.47
23:XX	1 (0.5)		1 (1.5%)		–
23:01	7 (3.5%)	2 (2.4%)	2 (3.0%)	3 (6.7%)	0.49
24:XX	8 (4.1%)	3 (3.7%)	5 (7.5%)		–
24:02	32 (16.5%)	18 (22.0%)	8 (11.9%)	6 (13.3%)	0.21
24:03	4 (2.0%)			4 (8.9%)	–
24:07	1 (0.5%)			1 (2.2%)	–
25:XX	1 (0.5%)	1 (1.2%)			–
25:01	13 (6.7%)	1 (1.2%)	10 (14.9)	2 (4.4%)	0.002**
26:XX	1 (0.5%)		1 (1.5%)		–
26:01	11 (5.7%)	5 (6.1%)	6 (9.0%)	2 (4.4%)	0.71
29:01	3 (1.5%)	2 (2.4%)		1 (2.2%)	–
29:02	5 (2.5%)	1 (1.2%)	3 (4.5%)	1 (2.2%)	0.45
30:XX	1 (0.5%)			1 (2.2%)	–
30:01	4 (2.0%)	2 (2.4%)	2 (3.0%)		–
30:02	1 (0.5%)	1 (1.2%)			–
31:01	2 (1.0%)	2 (2.4%)			–
32:XX	1 (0.5%)			1 (2.2%)	–
32:01	28 (14.4%)	15 (18.3%)	8 (11.9%)	5 (11.1%)	0.42
33:XX	1 (0.5%)		1 (1.5%)		–
33:01	5 (2.5%)	2 (2.4%)	1 (1.5%)	2(4.4%)	0.77
33:03	2(1.0%)	1 (1.2%)	1 (1.5%)		–
66:01	1 (0.5%)	1 (1.2%)			–
68:XX	1 (0.5%)	1 (1.2%)			–
68:01	6 (3.0%)	2 (2.4%)	3 (4.5%)	1 (2.2%)	0.77
68:02	3 (1.5%)		1 (1.5%)	2 (4.4%)	–
74:01	1 (0.5%)		1 (1.5%)		–

[(a)] observed frequency counts (%); [(b)] percentage out of 194 total; [(c)] percentage out of 82 total; [(d)] percentage out of 67 total; [(e)] percentage out of 45 total.

[(f)] for each allele observed in all the three groups, either asymptotic *Chi-square* test or *Fisher-exact* test was applied to investigate the statistical significance of observed differences in proportions, as appropriate.

** statistically highly significant differences ($p < 0.01$)

Table II b. The frequencies of HLA-B* allele identified within ALL, AML, and AA.

HLA-B* allele	Total[(a)(b)] (n=194)	ALL [(a)(c)] (n=82)	AML [(a)(d)] (n=67)	AA[(a)(e)] (n=45)	p-value [(f)]
–	4 (2.0%)	2 (2.4%)	1 (1.5%)	1 (2.2%)	–
07:XX	5 (2.6%)	2 (2.4%)	1 (1.5%)	2 (4.4%)	1
07:02	13 (6.7%)	4 (4.9%)	5 (7.5%)	4 (8.9%)	0.62
07:05	1 (05%)		1 (1.5%)		–
08:XX	2 (1.0%)	1 (1.2%)	1 (1.5%)		–
08:01	24 (12.4%)	8 (9.8%)	9 (13.4%)	7 (15.6%)	0.60
08:32	1 (05%)			1(2.2%)	–
13:XX	1 (05%)	1 (1.2%)			–
13:02	10 (5.2%)	3 (3.7%)	6 (9.0%)	1(2.2%)	0.31
14:01	2 (1.0%)		2 (3.0%)		–
14:02	17 (8.8%)	5 (6.1%)	6 (9.0%)	6 (13.3%)	0.39
15:XX	1 (05%)	1 (1.2%)			–
15:01	5 (2.6%)	4 (4.9%)	1 (1.5%)		–
15:02	1 (05%)			1 (2.2%)	–
15:18	3 (1.5%)	1 (1.2%)		2 (4.4%)	–
18:XX	5 (2.6%)	3 (3.7%)	2 (3.0%)		–
18:01	33 (17.0%)	14 (17.1%)	13 (19.4%)	6 (13.3%)	0.70
18:03	1 (05%)	1 (1.2%)			–
18:05	1 (05%)		1 (1.5%)		–
27:XX	1 (05%)		1 (1.5%)		–
27:02	5 (2.6%)	3 (3.7%)	1 (1.5%)	1 (2.2%)	0.85
27:05	9 (4.6%)	6 (7.3%)	1 (1.5%)	2 (4.4%)	0.25
35:XX	2 (1.0%)	1 (1.2%)	1 (1.5%)		–
35:01	22 (11.3%)	11 (13.4%)	9 (13.4%)	2 (4.4%)	0.25
35:02	8 (4.1%)	5 (6.1%)	2 (3.0%)	1 (2.2%)	0.59
35:03	16 (8.2%)	5 (6.1%)	2 (3.0%)	9 (20.0%)	0.006**
35:08	3 (1.5%)	2 (2.4%)	1 (1.5%)		–
37:XX	1 (05%)		1 (1.5%)		–
37:01	3 (1.5%)		1 (1.5%)	2 (4.4%)	–
38:01	14 (7.2%)	4 (4.9%)	6 (9.0%)	4 (8.9%)	0.56
39:XX	2 (1.0%)	1 (1.2%)	1 (1.5%)		–
39:01	3 (1.5%)	2 (2.4%)	1 (1.5%)		–
39:10	1 (05%)		1 (1.5%)		–
40:XX	4 (2.1%)		3 (4.5%)	1 (2.2%)	–
40:01	6 (3.1%)	2 (2.4%)	2 (3.0%)	2 (4.4%)	0.87
40:02	10 (5.2%)	4 (4.9%)	2 (3.0%)	4 (8.9%)	0.37
40:06	5 (2.6%)	3 (3.7%)	1 (1.5%)	1 (2.2%)	0.85
41:XX	1 (05%)		1 (1.5%)		–
41:01	4 (2.1%)	1 (1.2%)	2 (3.0%)	1 (2.2%)	0.83
41:02	1 (05%)	1 (1.2%)			–
44:XX	4 (2.1%)	3 (3.7%)	1 (1.5%)		–
44:02	18 (9.3%)	10 (12.2%)	5 (7.5%)	3 (6.7%)	0.57
44:03	6 (3.1%)	3 (3.7%)	1 (1.5%)	2 (4.4%)	0.66
44:05	6 (3.1%)	2 (2.4%)	2 (3.0%)	2 (4.4%)	0.87
44:27	1 (05%)	1 (1.2%)			–
45:01	1 (05%)			1 (2.2%)	–
45:04	1 (05%)		1 (1.5%)		–
47:01	3 (1.5%)		1 (1.5%)	2 (4.4%)	–
49:01	9 (4.6%)	4 (4.9%)	2 (3.0%)	3 (6.7%)	0.56
50:01	4 (2.1%)	2 (2.4%)	1 (1.5%)	1 (2.2%)	1

51:XX	2 (1.0%)			2 (4.4%)	–
51:01	32 (16.5%)	13 (15.9%)	14 (20.9%)	5 (11.1%)	0.38
51:09	1 (05%)	1 (1.2%)			–
52:XX	1 (05%)		1 (1.5%)		–
52:01	9 (4.6%)	7 (8.5%)		2 (4.4%)	–
52:05	1 (05%)	1 (1.2%)			–
53:XX	1 (05%)		1 (1.5%)		–
53:05	1 (05%)			1 (2.2%)	–
55:01	4 (2.1%)	2 (2.4%)	1 (1.5%)	1 (2.2%)	1
56:01	1 (05%)		1 (1.5%)		–
57:XX	2 (1.0%)	2 (2.4%)			–
57:01	5 (2.6%)	2 (2.4%)	2 (3.0%)	1 (2.2%)	1
58:XX	1 (05%)	1 (1.2%)			–
58:01	2 (1.0%)	1 (1.2%)	1 (1.5%)		–
78:XX	1 (05%)		1 (1.5%)		–

[(a)] observed frequency counts (%); [(b)] percentage out of 194 total; [(c)] percentage out of 82 total; [(d)] percentage out of 67 total; [(e)] percentage out of 45 total.

[(f)] for each allele observed in all the three groups, either asymptotic *Chi-square* test or *Fisher-exact* test was applied to investigate the statistical significance of observed differences in proportions, as appropriate.

** statistically highly significant differences ($p < 0.01$)

Table II c. The frequencies of HLA-C* allele identified within ALL, AML, and AA.

HLA-C* allele	**Total**[(a)(b)] (n=194)	**ALL** [(a)(c)] (n=82)	**AML** [(a)(d)] (n=67)	**AA**[(a)(e)] (n=45)	**p-value** [(f)]
–	13 (6.7%)	7 (8.5%)	4 (6.0%)	2 (4.4%)	–
01:02	8 (4.1%)	4 (4.9%)	4 (6.0%)		–
02:XX	2 (1.0%)		2 (3.0%)		–
02:02	35 (18.0%)	20 (24.4%)	6 (9.0%)	9 (20.0%)	0.047*
03:XX	2 (1.0%)	1 (1.2%)	1 (1.5%)		–
03:02	1 (0.5%)	1 (1.2%)			–
03:03	8 (4.1%)	4 (4.9%)	2 (3.0%)	2 (4.4%)	0.90
03:04	7 (3.6%)	3 (3.7%)	2 (3.0%)	2 (4.4%)	1
04:XX	2 (1.0%)	1 (1.2%)	1 (1.5%)		–
04:01	44 (22.7%)	20 (24.4%)	12 (17.9%)	12 (26.7%)	0.49
04:04	1 (0.5%)		1 (1.5%)		–
05:XX	2 (1.0%)		2 (3.0%)		–
05:01	15 (7.7%)	7 (8.5%)	5 (7.5%)	3 (6.7%)	1
06:XX	2 (1.0%)	1 (1.2%)	1 (1.5%)		–
06:02	25 (12.9%)	8 (9.8%)	9 (13.4%)	8 (17.8%)	0.43
07:XX	6 (3.1%)	2 (2.4%)	3 (4.5%)	1 (2.2%)	0.77
07:01	54 (27.8%)	20 (24.4%)	17 (25.4%)	17 (37.8%)	0.23
07:02	15 (7.7%)	5 (6.1%)	6 (9.0%)	4 (8.9%)	0.79
07:04	8 (4.1%)	5 (6.1%)	2 (3.0%)	1 (2.2%)	0.59
07:12	1 (0.5%)			1 (2.2%)	–
08:XX	1 (0.5%)		1 (1.5%)		–
08:01	1 (0.5%)			1 (2.2%)	–
08:02	18 (9.3%)	5 (6.1%)	8 (11.9%)	5 (11.1%)	0.39
12:XX	4 (2.1%)	2 (2.4%)	2 (3.0%)		–
12:02	16 (8.2%)	9 (11.0%)	4 (6.0%)	3 (6.7%)	0.50
12:03	30 (15.5%)	9 (11.0%)	14 (20.9%)	7 (15.6%)	0.25
14:XX	2 (1.0%)			2 (4.4%)	–

14:02	6 (3.1%)	3 (3.7%)	2 (3.0%)	1 (2.2%)	1
15:XX	1 (0.5%)	1 (1.2%)			–
15:02	17 (8.8%)	8 (9.8%)	6 (9.0%)	3 (6.7%)	0.90
15:05	2 (1.0%)	1 (1.2%)	1 (1.5%)		–
15:14	1 (0.5%)			1 (2.2%)	–
16:XX	1 (0.5%)		1 (1.5%)		–
16:01	2 (1.0%)	1 (1.2%)		1 (2.2%)	–
16:02	3 (1.5%)	1 (1.2%)	2 (3.0%)		–
16:04	1 (0.5%)	1 (1.2%)			–
17:01	2 (1.0%)	1 (1.2%)	1 (1.5%)		–

(a) observed frequency counts (%); (b) percentage out of 194 total; (c) percentage out of 82 total; (d) percentage out of 67 total; (e) percentage out of 45 total.

(f) for each allele observed in all the three groups, either asymptotic *Chi-square* test or *Fisher-exact* test was applied to investigate the statistical significance of observed differences in proportions, as appropriate.

* statistically significant differences ($p < 0.05$)

Table II d. The frequencies of HLA-DRB1* allele identified within ALL, AML, and AA.

HLA-DRB1* allele	**Total**(a)(b) (n=194)	**ALL**(a)(c) (n=82)	**AML** (a)(d) (n=67)	**AA**(a)(e) (n=45)	**p-value** (f)
–	3 (1.5%)	1 (1.2%)		2 (4.4%)	–
01:XX	2 (1.0%)	1 (1.2%)	1 (1.5%)		–
01:01	29 (14.9%)	12 (14.6%)	9 (13.4%)	8 (17.8%)	0.81
01:02	9 (4.6%)	4 (4.9%)	2 (3.0%)	3 (6.7%)	0.56
03:XX	2 (1.0%)	1 (1.2%)	1 (1.5%)		–
03:01	31 (16.0%)	13 (15.9%)	10 (14.9%)	8 (17.8%)	0.92
03:03	1 (0.5%)	1 (1.2%)			–
04:XX	3 (1.5%)	1 (1.2%)	1 (1.5%)	1 (2.2%)	1
04:01	12 (6.2%)	4 (4.9%)	4 (6.0%)	4 (8.9%)	0.69
04:02	4 (2.1%)	2 (2.4%)	2 (3.0%)		–
04:03	3 (1.5%)	1 (1.2%)		2 (4.4%)	–
04:04	5 (2.6%)	1 (1.2%)	1 (1.5%)	3 (6.7%)	0.16
04:05	2 (1.0%)	1 (1.2%)		1 (2.2%)	–
04:07	2 (1.0%)	1 (1.2%)	1 (1.5%)		–
04:10	1 (0.5%)			1 (2.2%)	–
07:XX	3 (1.5%)	2 (2.4%)	1 (1.5%)		–
07:01	26 (13.4%)	7 (8.5%)	14 (20.9%)	5 (11.1%)	0.077
08:01	5 (2.6%)	2 (2.4%)		3 (6.7%)	–
08:02	2 (1.0%)		1 (1.5%)	1 (2.2%)	–
09:01	2 (1.0%)	2 (2.4%)			–
10:01	2 (1.0%)	1 (1.2%)	1 (1.5%)		–
10:02	1 (0.5%)	1 (1.2%)			–
11:XX	12 (6.2%)	3 (3.7%)	9 (13.4%)		–
11:01	26 (13,4%)	12 (14.6%)	10 (14.9%)	4 (8.9%)	0.60
11:02	1 (0.5%)	1 (1.2%)			–
11:03	3 (1.5%)		3 (4.5%)		–
11:04	34 (17.5%)	21 (25.6%)	9 (13.4%)	4 (8.9%)	0.033*
11:61	1 (0.5%)		1 (1.5%)		–
12:XX	2 (1.0%)	1 (1.2%)	1 (1.5%)		–
12:01	6 (3.1)	4 (4.9%)	1 (1.5%)	1 (2.2%)	0.57
13:XX	3 (1.5%)	2 (2.4%)	1 (1.5%)		–
13:01	22 (11.3%)	6 (7.3%)	8 (11.9%)	8 (17.8%)	0.20

13:02	5 (2.6%)	3 (3.7%)	2 (3.0%)		–
13:03	4 (2.1%)	1 (1.2%)	3 (4.5%)		–
13:05	1 (0.5%)	1 (1.2%)			–
13:68	1 (0.5%)	1 (1.2%)			–
14:XX	1 (0.5%)		1 (1.5%)		–
14:01	6 (7.3%)	3 (3.7%)	1 (1.5%)	2 (4.4%)	0.66
14:02	1 (0.5%)	1 (1.2%)			–
14:04	5 (2.6%)	2 (2.4%)	2 (3.0%)	1 (2.2%)	1
14:07	1 (0.5%)	1 (1.2%)			–
14:54	7 (3.6%)	4 (4.9%)	3 (4.5%)		–
15:XX	2 (1.0%)		1 (1.5%)	1 (2.2%)	–
15:01	16 (8.2%)	4 (4.9%)	6 (9.0%)	6 (13.3%)	0.23
15:02	9 (4.6%)	6 (7.3%)		3 (6.7%)	–
15:07	1 (0.5%)			1 (2.2%)	–
16:XX	4 (2.1%)	2 (2.4%)	1 (1.5%)	1 (2.2%)	1
16:01	30 (15.5%)	14 (17.1%)	11 (16.4%)	5 (11.1%)	0.65
16:02	7 (3.6%)	5 (6.1%)	1 (1.5%)	1 (2.2%)	0.28

[a] observed frequency counts (%); [b] percentage out of 194 total; [c] percentage out of 82 total; [d] percentage out of 67 total; [e] percentage out of 45 total.

[f] for each allele observed in all the three groups, either asymptotic *Chi-square* test or *Fisher-exact* test was applied to investigate the statistical significance of observed differences in proportions, as appropriate.

*statistically significant differences ($p < 0.05$)

Table II e. The frequencies of HLA-DQB1* allele identified within ALL, AML, and AA.

HLA-DQB1* allele	**Total**[a][b] (n=194)	**ALL**[a][c] (n=82)	**AML** [a][d] (n=67)	**AA**[a][e] (n=45)	**p-value** [f]
–	3 (1.5%)	3 (3.7%)			–
02:XX	4 (2.1%)	2 (2.4%)	2 (3.0%)		–
02:01	33 (17.0%)	13 (15.9%)	10 (14.9%)	10 (22.2%)	0.56
02:02	21 (10.8%)	5 (6.1%)	12 (17.9%)	4 (8.9%)	0.022*
03:XX	16 (8.2%)	5 (6.1%)	10 (14.9%)	1 (2.2%)	0.05#
03:01	75 (38.7%)	37 (45.1%)	25 (37.3%)	13 (28.9%)	0.19
03:02	21 (10.8%)	8 (9.8%)	4 (6.0%)	9 (20.0%)	0.075
03:03	8 (4.1%)	3 (3.7%)	3 (4.5%)	2 (4.4%)	1
03:05	1 (0.5%)	1 (1.2%)			–
04:01	1 (0.5%)		1 (1.5%)		–
04:02	8 (4.1%)	2 (2.4%)	2 (3.0%)	4 (8.9%)	0.24
05:XX	12 (6.2%)	5 (6.1%)	6 (9.0%)	1 (2.2%)	0.38
05:01	32 (16.5%)	16 (19.5%)	10 (14.9%)	6 (13.3%)	0.61
05:02	36 (18.6%)	19 (23.2%)	11 (16.4%)	6 (13.3%)	0.34
05:03	16 (8.2%)	8 (9.8%)	4 (6.0%)	4 (8.9%)	0.71
05:04	3 (1.5%)			3 (6.7%)	–
05:05	1 (0.5%)	1 (1.2%)			–
06:XX	7 (3.6%)	5 (6.1%)	1 (1.5%)	1 (2.2%)	0.34
06:01	6 (3.1%)	3 (3.7%)		3 (6.7%)	–
06:02	16 (8.2%)	5 (6.1%)	6 (9.0%)	5 (11.1%)	0.57
06:03	23 (11.9%)	6 (7.3%)	8 (11.9%)	9 (20.0%)	0.11
06:04	4 (2.1%)	2 (2.4%)	2 (3.0%)		–
06:11	1 (0.5%)			1 (2.2%)	–
06:18	1 (0.5%)		1 (1.5%)		–

[a] observed frequency counts (%); [b] percentage out of 194 total; [c] percentage out of 82 total; [d] percentage out of 67 total; [e] percentage out of 45 total.

[f] for each allele observed in all the three groups, either asymptotic *Chi-square* test or *Fisher-exact* test was applied to investigate the statistical significance of observed differences in proportions, as appropriate.

* statistically significant differences ($p < 0.05$); # marginally statistical significance ($p \approx 0.05$)

Table III (a and b) show the most frequent haplotypes of class I and class II HLA allele, respectively.

According to haplotypes analysis, A*02:01 B*18:01 C*07:01 and A*01:01 B*08:01 C*07:01 in AML patients, A*02:01 B*35:03 C*04:01 in ALL and in AA patients, frequencies were significantly high for class I HLA (7.5%, 4.5% 3.7%. and 6.7%, respectively). The most frequent haplotypes of class II HLA allele were DRB1*11:04 DQB1*03:01 (22.0%) in ALL, DRB1*03:01 DQB1*02:01 and DRB1*11:01 DQB1*03:01 in AML and DRB1*03:01 DQB1*02:01 in AA.

According to haplotypes analysis, A*02:01 B*18:01 C*07:01 and A*01:01 B*08:01 C*07:01 in AML patients, A*02:01 B*35:03 C*04:01 in ALL and in AA patients, frequencies were significantly high for class I HLA (7.5%, 4.5% 3.7%. and 6.7%, respectively). The most frequent haplotypes of class II HLA allele were DRB1*11:04 DQB1*03:01 (22.0%) in ALL, DRB1*03:01 DQB1*02:01 and DRB1*11:01 DQB1*03:01 in AML and DRB1*03:01 DQB1*02:01 in AA.

Table III a. The most frequent haplotypes of class I HLA allele identified within ALL, AML, and AA.

HLA-A* B* C*	Total[a][b] (n=194)	ALL[a][c] (n=82)	AML[a][d] (n=67)	AA[a][e] (n=45)	p-value[f]
A*01:01 B*08:01 C*07:01	7 (3.6%)	2 (2.4%)	3 (4.5%)	2 (4.4%)	0.69
A*02:01 B*35:03 C*04:01	7 (3.6%)	3 (3.7%)	1 (1.5%)	3 (6.7%)	0.425
A*02:01 B*18:01 C*07:01	6 (3.1%)	1 (1.2%)	5 (7.5%)	–	0.059
A*01:01 B*08:01 C*02:02	3 (1.5%)	–	1 (1.5%)	2 (4.4%)	0.106
A*01:01 B*08:01 C*04:01	3 (1.5%)	2 (2.4%)	–	1 (2.2%)	0.454
A*02:01 B*13:02 C*06:02	3 (1.5%)	1 (1.2%)	2(3.0%)	–	0.606

[a] observed frequency counts (%); [b] percentage out of 194 total; [c] percentage out of 82 total; [d] percentage out of 67 total; [e] percentage out of 45 total.

[f] for each haplotype, either asymptotic *Chi-square* test or *Fisher-exact* test was applied to investigate the statistical significance of observed differences in proportions, as appropriate.

Table III b. The most frequent haplotypes of class II HLA allele identified within ALL, AML, and AA.

HLA-DRB1* DQB1*	Total[a][b] (n=194)	ALL[a][c] (n=82)	AML[a][d] (n=67)	AA[a][e] (n=45)	p-value[f]
DRB1*11:04 DQB1*03:01	28 (14.4%)	18 (22.0%)	8 (11.9%)	2 (4.4%)	0.021*
DRB1*03:01 DQB1*02:01	25 (12.9%)	9 (11.0%)	9 (13.4%)	7 (15.6%)	0.752
DRB1*11:01 DQB1*03:01	20 (10.3%)	8 (9.8%)	9 (13.4%)	3 (6.7%)	0.547
DRB1*16:01 DQB1*05:02	20 (10.3%)	10 (12.2%)	6 (9.0%)	4 (8.9%)	0.832
DRB1*07:01 DQB1*02:02	17 (8.8%)	3 (3.7%)	10 (14.9%)	4 (8.9%)	0.041*
DRB1*01:01 DQB1*05:01	15 (7.7%)	6 (7.3%)	5 (7.5%)	4 (8.9%)	0.943
DRB1*13:01 DQB1*06:03	13 (6.7%)	3 (3.7%)	4 (6.0%)	6 (13.3%)	0.134

[a] observed frequency counts (%); [b] percentage out of 194 total; [c] percentage out of 82 total; [d] percentage out of 67 total; [e] percentage out of 45 total.
[f] for each haplotype, either asymptotic *Chi-square* test or *Fisher-exact* test was applied to investigate the statistical significance of observed differences in proportions, as appropriate.
* statistically significant differences ($p < 0.05$);

The inter-haplotype correlation analysis was applied, with results in Table IV. The highly significant correlations were emphasized in bold, though all the significant correlation values were marked as well. The Bartlett's test of sphericity was highly significant ($p< 0.001$), so the Principal Component Analysis (PCA) was subsequently applied.

Table IV. Inter-haplotypes correlations. Highly significant correlations are in bold.

	HLA haplotype	(i)	(ii)	(iii)	(iv)	(v)	(vi)	(vii)	(viii)	(ix)	(x)	(xi)	(xii)	(xiii)
(i)	A*01:01 B*08:01 C*07:01	1.0	-.037	-.035	-.024	-.024	-.024	-.079	**.256****	-.066	-.066	-.060	-.056	-.052
(ii)	A*02:01 B*35:03 C*04:01		1.0	-.035	-.024	-.024	-.024	**.235****	.008	-.066	.025	-.060	-.056	-.052
(iii)	A*02:01 B*18:01 C*07:01			1.0	-.022	-.022	**.219****	**.181****	-.069	.037	.037	.155*	-.052	-.048
(iv)	A*01:01 B*08:01 C*02:02				1.0	-.016	-.016	-.051	**.326****	.095	-.042	-.039	.120	-.034
(v)	A*01:01 B*08:01 C*04:01					1.0	-.016	.067	**.201****	-.042	-.042	.109	-.036	-.034
(vi)	A*02:01 B*13:02 C*06:02						1.0	**.186****	-.048	.095	-.042	**.404****	-.036	-.034
(vii)	DRB1*11:04 DQB1*03:01							1.0	.017	.005	.102	.080	-.009	.066
(viii)	DRB1*03:01 DQB1*02:01								1.0	.123*	-.130*	-.065	-.054	-.103
(ix)	DRB1*11:01 DQB1*03:01									1.0	-.059	.075	-.098	.045
(x)	DRB1*16:01 DQB1*05:02										1.0	.015	-.098	-.091
(xi)	DRB1*07:01 DQB1*02:02											1.0	-.090	-.083
(xii)	DRB1*01:01 DQB1*05:01												1.0	.077
(xiii)	DRB1*13:01 DQB1*06:03													1.0

Kaiser-Meyer-Olkin measure = 0.492

Bartlett's test of sphericity: Chi-square=163.212 (df=78), p<0.001

Statistical significance: * p<0.05; ** p<0.01

Table V presents the PCA results. Based on the scree plot (Figure 1) and the criterion of eigenvalues greater than 1, seven factors were extracted explaining more than 68% of the total variance. For each extracted factor, the main contributive haplotypes are emphasized in bold. The haplotypes' patterns of the factors for the three types of anemia proved to be indistinct. Figure 2 shows the matrix of the two-factor correlations for the three blood condition diseases. Nevertheless, the seven factors account for the structure analysis of the frequently observed haplotypes, as shown in the diagram constructed based on data in Table 5 and Figure 3.

Table V. Principal component analysis (PCA) and factor loading for the HLA haplotypes.
The main contributive haplotypes for each factor are in bold.

	Extracted factors						
HLA haplotype	**F1**	**F2**	**F3**	**F4**	**F5**	**F6**	**F7**
A*01:01 B*08:01 C*07:01	-.269	.320	.179	**-.378**	.177	-.237	**.591**
A*02:01 B*35:03 C*04:01	.083	-.117	**.647**	**.372**	-.064	-.128	.131
A*02:01 B*18:01 C*07:01	**.533**	.104	-.035	.032	-.090	.102	.294
A*01:01 B*08:01 C*02:02	-.265	**.499**	-.102	**.384**	-.338	**.398**	.001
A*01:01 B*08:01 C*04:01	.024	.341	.233	-.015	**.580**	.057	**-.593**
A*02:01 B*13:02 C*06:02	**.680**	.284	-.209	.025	.090	.028	.224
DRB1*11:04 DQB1*03:01	**.465**	.020	**.436**	**.508**	.078	-.112	.082
DRB1*03:01 DQB1*02:01	-.333	**.756**	.241	.097	-.007	-.036	.015
DRB1*11:01 DQB1*03:01	.118	**.360**	-.298	.138	**-.514**	**-.415**	-.248
DRB1*16:01 DQB1*05:02	.191	-.286	**.355**	-.196	**-.409**	.303	-.207
DRB1*07:01 DQB1*02:02	**.646**	.282	-.188	-.189	.165	.121	-.107
DRB1*01:01 DQB1*05:01	-.209	-.139	-.325	**.465**	.283	**.490**	.222
DRB1*13:01 DQB1*06:03	-.064	-.238	-.329	**.434**	.187	**-.519**	-.053
Eigenvalue	1.738	1.511	1.272	1.195	1.082	1.047	1.030
Variance (%)	13.367%	11.626%	9.783%	9.190%	8.324%	8.054%	7.921%
Cumulative of variance (%)	13.367%	24.992%	34.775%	43.966%	52.290%	60.344%	68.265%

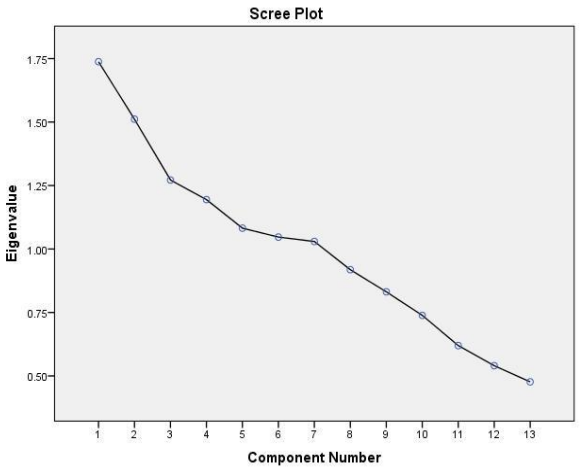

Fig. 1. The scree plot for the 13 most frequent haplotypes considered in the principal component analysis (PCA). Based on the criterion of eigenvalue >1, seven factors were chosen, accounting for more than 68% of the total variance.

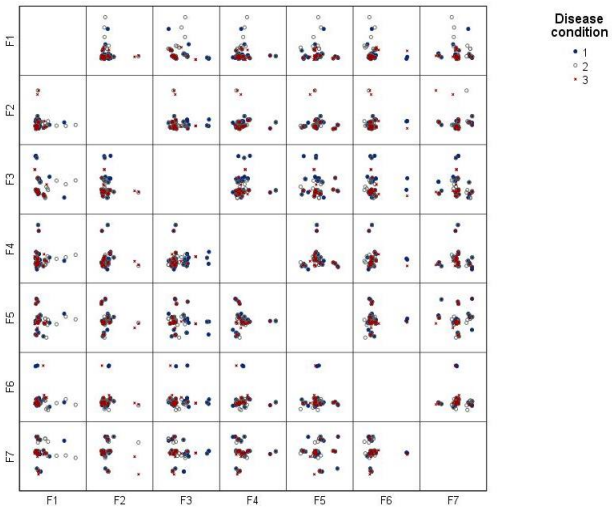

Fig. 2. Matrix of the two-factor correlations for the three blood condition diseases: 1 – ALL, 2 – AML, 3 – AA. F1 to F7 are the seven factors resulted from the principal component analysis (PCA).

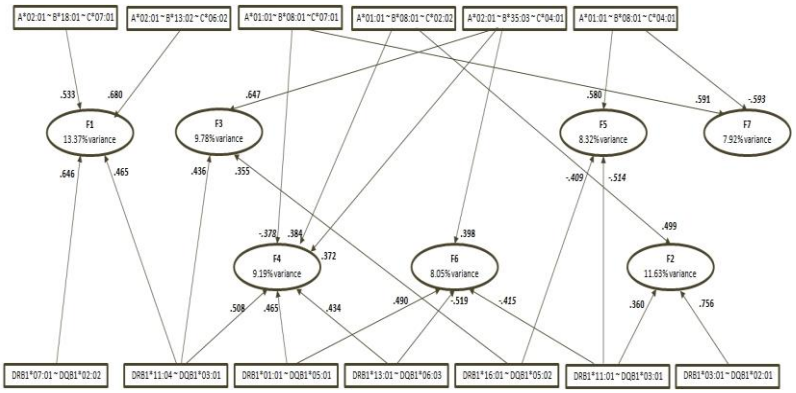

Fig. 3. Diagram of the underlying structure of frequently observed haplotypes within the three blood conditions analyzed, based on the seven factors resulted from the principal component analysis (PCA).

CONCLUSIONS

This study found that the most frequent haplotypes in a studied population group of 194 patients with one of the three disorders analyzed (ALL, AML, and AA) were A*02:01 B*13:02 C*06:02 DRB1*07:01 DQB1*02:02, A*01:01 B* 08:01 C*02:02 DRB1*03:01 DQB1*02:01, A*01:01 B*08:01 C*07:01 DRB1*03:01 DQB1*02:01, A*02:01 B*35:03 C*04:01 DRB1*11:04 DQB1*03:01, A*02:01 B*13:02 C*06:02 DRB1*11:04 DQB1*03:01 and A*02:01 B*18:01 C*07:01 DRB1*11:04 DQB1*03:01.

The analysis of the study shows that there is no haplotype to be considered a risk factor in the development of a haematological disease, but these results can be further used in a larger study.

The most common alleles susceptibile to be considered as a risk factor in the development of hematological diseases in patients in the western part of Romania are A*02:01 in AA but also ALL, A*24:02 in ALL, B*18:01 in AML but also ALL and AA, B*08:01 in AA, C*02:02 in ALL, C*04:01 in ALL and AML, DRB1*03:01 in AA and ALL, DRB1*07:01 in AML, DRB1*11:04 in ALL, DQB1*03:01 in ALL and AML.

ACKNOWLEDGMENTS

This work was supported by the National Transplant Program.

REFERENCES

1. Neefjes J, Jongsma MLM, Paul P, Bakke O. Towards a systems understanding of MHC class I and MHC class II antigen presentation," *Nat. Rev. Immunol.*, 2011; 11: 823-836.
2. Benacerraf B. Role of MHC gene products in immune regulation. *Science 2006;* 212(4500): 1229-1238.
3. Ozdilli K, Oguz FS, Anak S, Kekik C, Carin M, Gedikoglu G. The frequency of HLA class I and II alleles in turkish childhood acute leukaemia patients. *J. Int. Med. Res.*, 2010; 38(5): 1835-1844.
4. Janeway CA Jr, Travers P, Walport M, et al. The Major Histocompatibility Complex and Inflammation, in *Immunobiology: The Immune System in Health and Disease*, 5th Ed., New York: Garland Science, 2001.
5. Marsh SGE, *et al.* Nomenclature for factors of the HLA system. *Tissue Antigens*, 2010; 75(4): 291-455.
6. Matzaraki V, Kumar V, Wijmenga C, Zhernakova A. The MHC locus and genetic susceptibility to autoimmune and infectious diseases. *Genome Biol.*, 2017; 18(1): 76.
7. Wieczorek M, *et al.* Major Histocompatibility Complex (MHC) Class I and MHC Class II Proteins: Conformational Plasticity in Antigen Presentation. *Front. Immunol.*, 2017; 8: 292.
8. Fernández-Torres J, Flores-Jiménez D, Arroyo-Pérez A, Granados J, López-Reyes A. HLA-B*40 Allele Plays a Role in the Development of Acute Leukemia in Mexican Population: A Case-Control Study. *Biomed Res. Int.*, 2013; 2013; 1-6.
9. Patiroglu T, Akar HH. Relationships of Human Leukocyte Antigen-A, -B, -DRB1 Alleles, and Haplotypes in 129 Ethnic Turkish Patients With Acute Myeloblastic Leukemia. *Lab. Med.*, 2015; 46(3): 195-199.
10. Pui CH, Carroll WL, Meshinchi S, Arceci RJ. Biology, Risk Stratification, and Therapy of Pediatric Acute Leukemias: An Update. *J. Clin. Oncol.*, 2011; 29(5): 551-565.
11. Schroter S, Plowman R, Hutchings A, Gonzalez A. Reporting ethics committee approval and patient consent by study design in five general medical journals. *J. Med. Ethics*, 2006; 32(12): 718–23.
12. Robinson J, Mistry K, McWilliam H, Lopez R, Marsh SGE. IPD--the Immuno Polymorphism Database. *Nucleic Acids Res.*, 2010; 38: D863-9.
13. Robinson J, Halliwell JA, McWilliam H, Lopez R, Parham P, Marsh SGE. The IMGT/HLA database. *Nucleic Acids Res.*, 2013; 41: D1222-7.
14. Hansen AM, Jeske D, Kirsch W. A Chi-Square Goodness-of-Fit Test for Autoregressive Logistic Regression Models with Applications to Patient Screening. *J. Biopharm. Stat.*, 2015; 25(1): 89-108.
15. Bergh D. Chi-Squared Test of Fit and Sample Size-A Comparison between a Random Sample Approach and a Chi-Square Value Adjustment Method. *J. Appl. Meas.*, 2015; 16(2): 204-17.
16. Chen Q, Wang W, Lin P, Zhong Q, Yu S. Application of Excel programs of Fisher exact probability test for medical data. *Nan Fang Yi Ke Da Xue Xue Bao*, 2009; 29(4): 791-3.

B*08:01 HLA CLASA I, ALELELE MHC CLASA II ȘI FRECVENȚA HAPLOTIPURILOR LA PACIENȚII CU AFECȚIUNI HEMATOLOGICE ÎN VESTUL ROMÂNIEI

REZUMAT

Studiul de față s-a desfășurat între 2015 și 2018, având ca scop investigarea incidenței haplotipurilor în leucemia acută limfoblastică (ALL), leucemia acută mieloidă (AML) și anemia aplastică (AA) în partea de vest a României. A fost utilizată tehnica de secvențializare de tip SBT (sequencing-based typing), folosind kiturile SeCore ONE LAMBDA, cu ajutorul cărora au fost tipizate genele HLA clasa I și II. Ulterior, a fost analizată și comparată frecvența alelelor pentru bolile hematologice.

Cuvinte cheie: gene HLA clasa I și II, leucemie acută limfoblastică (ALL), leucemie acută mieloidă (AML), anemie aplastică (AA), tehnica de tipizare prin secvențiere (SBT)

EXPERIMENTAL ELECTROCARDIOGRAPH FOR TELEMEDICINE

FLORIN ȘUȘMAN[1], MIHAELA LASCU[1], VALENTIN ORDODI[1,2]

[1]Politehnica University of Timișoara, 2 Victoriei Square, RO-300006, Timișoara, România
[2]OncoGen Research Center, Pius Brânzeu Clinical Emergency Hospital, 156 Liviu Rebreanu Bv, RO-300723, Timișoara, România.

ABSTRACT
This article describes a simple electrocardiographic device that allows via the mobile phone network the real-time monitoring of the electrocardiogram at the patient's home. The experimental device is realized by coupling some miniature electronic modules, it is powered by a 9 V alkaline battery which gives it a long operating autonomy and which allows the recording of a standard ECG derivation. The electrocardiogram is transmitted in real time through a wireless device to the patient's mobile phone. It has the possibility to save the respective recording, to transmit it to the cardiologist or to the family physician, either in real time or at a later date, through appropriate software.
Key words: ECG machine, mobile phone network, telemedicine

INTRODUCTION

Cardiovascular disease is currently the leading cause of morbidity and mortality worldwide. Countries with a high standard of living have a true epidemic of cardiovascular diseases, especially ischemic. The sudden death of these patients is quite difficult to avoid in medical practice, as it is due in most cases to heart rhythm disorders that are most often electrocardiographic [1,2,3]. Telemedicine, a seemingly new branch of medicine, involves remote physician-patient communication [4]. The main contribution of the present telemedicine is the monitoring of some physiological and biochemical parameters of the human body and the transmission of the data collected through an electronic system of remote communications to the specialist doctor. Cardiology benefits greatly from the development of these technologies, the essential cardiovascular parameters: peripheral pulse, oxygen saturation, blood pressure, electrocardiogram, being easy to record with the usual electronic devices and thus the patient can transmit this data to the doctor in a very simple way from home [5,6,7]. The first remote transmissions of an electrocardiogram were made more than half a century ago. Currently, the existing technologies both in terms of the acquisition and amplification of the ECG signal as well as the analogical numerical conversion of the data, respectively their transmission via mobile telephony, make this mode of consultation widely used [8,9].

Experimental device

The experimental device acquires, amplifies and processes, displays and transmits the ECG signal to a mobile phone via Bluetooth device. The electrocardiogram is sent in real time through a specialized software to the cardiologist or can be saved on the mobile device and sent later or archived. The power supply of the experimental device is provided by a 9 V alkaline battery. In figure 1 we can see the modules from which the device is made.

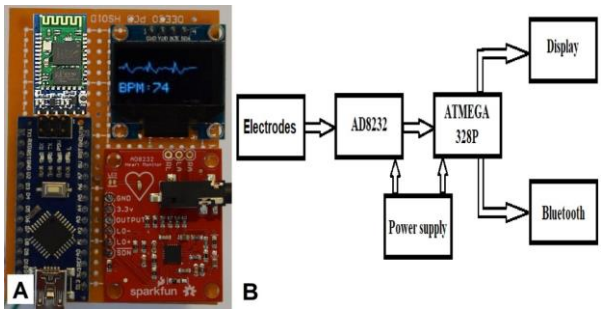

Fig.1. A. Experimental device (overview); **B.** Block diagram

Received August 20th 2019. Accepted October 12th 2019. Address for correspondence: Valentin Ordodi, PhD, Politehnica University of Timișoara, 2 Victoriei Square, RO-300006, Timișoara, România; phone: +40-256-404219; e-mail: vali.medtm99@gmail.com

- The acquisition and amplification module of the ECG signal. AD8232 is an integrated circuit whose design is specific to ECG applications, but also to other applications that use biopotential measurements. It has been modeled to extract, amplify and filter small biopotential signals under noise conditions. This design incorporates a very low power ADC converter along with an integrated µC for easy signal acquisition. The configuration used in the experimental device uses the D_{II} derivation because in most individuals the amplitude of the waves in this derivation is maximum (the projection of the cardiac electric vector in the Einthoven triangle) [10].
- High-performance picoPower microchip microcontroller (Atmega 328p), based on 8-bit AVR RISC, combines ISP flash memory with 32KB memory with real-time write capabilities, EEPROM 1024B, SRK 2KB, 23 general-purpose I / O lines, 32 purpose work registers general, / counters with comparison modes, internal and external switches, USART programmable serial, two-wire serial interface, SPI serial port, 10-bit 6-channel A / D converter , programmable monitoring timer with internal oscillator and five selectable energy saving modes [11].
- Display is a blue light OLED type, of 0.96 inch. It is having a resolution of 128x64. OLED is a self light-emitting technology composed of a thin, multi-layered organic film placed between an anode and cathode. In contrast to LCD technology, OLED does not require a backlight. The display module can be interfaced with any microcontroller using IIC protocols [12].
- Bluetooth module is HC-06 type. This module performs the wireless connection between the experimental device and the mobile phone. Is an Arduino compatible device that establishes a bilateral serial connection on the 2.4 GHz frequency [13].

The programming interface used to design the software is Arduino IDE and is based on the C / C ++ language. Also through Arduino IDE the driver for the OLED display was downloaded [14].

RESULTS AND DISCUSSION

A preliminary experiment using the proposed experimental device was performed on a male subject 24 years old. The bipolar DII standard derivation of the limbs was recorded, connecting the negative pole of the instrumentation amplifier at the level of the right shoulder, and the positive one at the thoracic level in the spinal projection area. Thus the cardiac electric vector will have a maximum representation, and the recorded electrocardiographic signal will be maximum. The connection between the experimental device and the mobile phone is established via Bluetooth, the graphical application is launched and the electrocardiogram is followed in real time. Figure 2 shows the appearance of this recording on the mobile phone.

Fig. 2. Electrocardiogram viewed on the mobile phone

The heart rate and the ECG aspect are transmitted in real time to the cardiologist, using the appinventor.mit.edu application available online. Also the recordings can be stored in the memory of the mobile phone and compared later [15].

CONCLUSIONS

The presented experimental device is simple, inexpensive, very accessible and easy to use by most patients. The recorded electrocardiogram corresponds qualitatively to the requirements for a correct diagnosis in the case of rhythm disorders, and even of ischemic episodes, which recommends it for monitoring the cardiac activity at home and transmitting data directly to the attending physician. The patient's safety is ensured by the use of a 9 V battery. There is absolutely no physical connection between the experimental device and another electronic device: computer, cable telephone line, etc., avoiding the risk of accidents.

REFERENCES

1. Bunu C. *Fiziologia aparatului cardiovascular*. Ed. Orizonturi Universitare, Timișoara, 2003.
2. Noveanu L, Mihalaș G. *Fiziologie Practică. Vol II*. Ed. Mirton Timișoara, 2005.
3. Diaconu C. Explorări funcționale în medicina internă. Ed. All, București, 2016.
4. Bashshur RL, Armstrong PA, and Youssef 21, *Telemedicine;* Explorations in the use of telecommunications in health care, Charles C. Thomas, Springfield, IL, 1975.
5. Economakos G, Nikolaidis L, and Papakonstantinou G. Animation techniques for real time ECG monitoring, in

Computers in Cardiology *1998,* Cleveland, OH, USA, September 1998, IEEE.
6. Brunetti ND, De Gennaro L, Dellegrottaglie G, Amoruso D,Antonelli G, Di Biase M. A regional prehospital electrocardio-gram network with a single telecardiology ''hub'' for public emergency medical service: technical requirements, logis-tics, manpower, and preliminary results. *Telemed J E Health*, 2011; 17: 72-33.
7. Brunetti ND, Dellegrottaglie G, Di Giuseppe G, LoprioreC, Gardini G, Patruno S, et al. YOUng Football Italianamateur players Remote electrocardiogram Screening with Telemedicine (YOU FIRST) study: preliminary results. *Int J Cardiol*, 2014; 176: 1257-8.
8. Woodward B,Istepanian RH,Richards C.Design of telemedicine system using a mobile telephone. IEEE Transactions on Information Technology in Biomedicine, 2001; 5(1):13-16.
9. Chang CC, Yang YC, Teng WC, et al. An SCP compatible 12-lead electrocardiogram database for signal transmission, storage and analysis. *J Computer in Cardiology*, 2004, 31:621-624.
10. www.analog.com/media/en/technical-documentation/data-sheets/ad8232.pdf
11. www.microchip.com/downloads/en/DeviceDoc/Atmel-7810-Automotive-Microcontrollers-ATmega328P_Datasheet.pdf
12. http://www.farnell.com/datasheets/1718446.pd
13. https://www.olimex.com/Products/Components/RF/BLUETOOTH-SERIAL-HC-06/resources/hc06.pdf
14. https://www.arduino.cc/en/main/software
15. http://appinventor.mit.edu

DISPOZITIV ELECTROCARDIOGRAFIC PENTRU TELEMEDICINĂ

REZUMAT
În prezentul articol este descris un dispozitiv electrocardiografic simplu, care permite via reteaua de telefonie mobila monitorizarea in timp real a electrocardiogramei la domiciliul pacientului. Dispozitivul experimental este realizat prin cuplarea unor module electronice miniaturale, este alimentat de la o baterie alcalina de 9 V ceea ce ii confera o autonomie de functionare indelungata si care permite inregistrarea unei derivatii ECG standard. Electrocardiograma este transmisa in timp real prin intermediul unui dispozitiv fara fir catre telefonul mobil al pacientului. Acesta are posibilitatea sa salveze inregistrarea respectiva, sa o transmita medicului specialist cardiolog sau medicului de familie, fie in timp real fie la o data ulterioara prin intermediul unei software adecvat.
Cuvinte cheie: dispozitiv ECG, rețea de telefonie mobilă, telemedicină

EGF-INDUCED CHEMOTAXIS OF SK-BR3 TUMOR CELLS *IN VITRO* USING HOLOGRAPHIC IMAGING

DANA PLEȘCA[1], DANIELA CRÎSNIC[1,2,3], DACIANA NISTOR[1,2], CARMEN TATU[1,2], GABRIELA TANASIE[1,2], ROXANA ZOGOREAN[2], SIMONA ANGHEL[1,2], OANA GAVRILIUC[1,2], FLORINA BOJIN[1,2], VIRGIL PĂUNESCU[1,2]

[1]Department of Functional Sciences, „Victor Babes" University of Medicine and Pharmacy Timisoara, Romania
[2]OncoGen-Centre for Gene and Cellular Therapies in the Treatment of Cancer, „Pius Brinzeu" Clinical Emergency County Hospital Timisoara, Romania
[3]SC Biodim SRL, 59 Porumbescu St, RO-300239, Timișoara, România

ABSTRACT

In this study we evaluated the ability for induction of chemotaxia *in vitro*, for a tumor cell line of breast adenocarcinoma, SK-BR3. This cell line was evaluated for the morphological and phenotypic characteristics, and for expression of receptors involved in chemotaxis. SK-BR3 cell line expresses epidermal growth factor receptor (EGFR), so that we used EGF (epidermal growth factor) in our studies, as chemotaxis inducer. Chemotaxis was studied in specific μ-slides, using a holographic imaging system – Holomonitor M4.

From the morphological point of view, tumor cells have a polygonal shape, with a cellular size of 15-20 μm. The chemotactic effects of EGF on SK-BR3 were evaluated by motility, migration and migration speed, parameters which were monitored for 24 hours. Cultured on fibronectin-coated plates, SK-BR3 cells in presence of EGF exhibited an increased motility compared to native SK-BR3 (818.1 $\mu m \pm$ sd, and 673.7 $\mu m \pm$ sd, respectively). Migration speed is 2 times higher for the tumor cells in presence of EGF, while the migration is similar, but is unidirectional.

This in vitro study is very important for invasion and tumor metastasis and provides a targeted image about these processes for SK-BR3 tumor cell line, mainly due to the investigation methods using Holomonitor M4 and holographic images analysis by Hstudio software. These investigations could be further extended to analysis of other tumor cells and several different chemotaxis inducers.

Key words: chemotaxia, tumor cells, Holomonitor M4, EGF

INTRODUCTION

Chemotaxis represents directed cellular movement in response to a chemical gradient from the extracellular environment. The process is important for initiation and maintenance of the inflammatory processes, while in cancer it accounts for tumor cells dissemination and probably distant metastases. In tumors, chemotaxis of carcinoma cells and stromal cells is mediated by chemokines, chemokine receptors, growth factors and growth factors receptors, some of them presented in Table I [1]. Tumor cells can move both randomly and directionally, efficient migration being accomplished when cells have directed movement [2].

For chemotactic movement, cells should pass through three individual steps: sensing the chemical compound, polarization and locomotion. Single tumor cells are involved in two different types of directed movement: amoeboid and mesenchymal migration. In our study, we were interested in the mesenchymal type of tumor cell migration, which is characterized by elongated cellular morphology, establishing cellular polarity and low velocity of migration (0.1-1 μm/min) (Table II) [3]. Mesenchymal migration is also a characteristic of most carcinomas or cells undergoing epithelial to mesenchymal transition (EMT) [4-9]. However, amoeboid and mesenchymal migration can interconvert, both *in vivo* and *in vitro*.

Received 12th of October 2019. Accepted 11th of November 2019. Address for correspondence: Florina Bojin, MD, PhD, Department of Functional Sciences, „Victor Babes" University of Medicine and Pharmacy Timisoara, Eftimie Murgu Square No. 2A, RO-300041, Romania; phone/fax: +40256490507; e-mail: florinabojin@umft.ro

Signaling regulation is very important for chemotaxis of tumor cells, thus making important studying chemotaxis in physiological relevant conditions, within the tumor microenvironment. Several studies showed that a complex chemokine network initiates and regulates chemotaxis of tumor cells. This network can also regulate several other intracellular processes, such as tumor development, angiogenesis, tumor evasion, senescence, survival and metastatic progression, at this moment more than 50 different chemokines and chemokine receptors being involved in cancer, and more than 30% of them being also involved in chemotaxis.

Table I. Growth factors involved in cancer cells chemotaxia

Chemokines and growth factors	Receptors	Experimental data	Cancer types
EGF, TGFa, betacellulin, HBEGF	EGFR (ERBB1), ERBB2 (Her2), ERBB3 and ERBB4	Transwell assay 3D invasion *In vivo* invasion Intravital imaging	Breast, lung, colorectal, gastric cancers, glioblastoma
FGF	FGFR1-4	Transwell assay	Breast, ovarian, pancreatic, renal cancers, glioblastoma
PDGF	PDGFR	Transwell assay 3D culture	Breast cancer, glioblastoma, melanoma
TGFβ	TGFβR1 and TGFβR2	Transwell assay Wound-healing assay Intravital imaging	Breast, lung, squamous cell and oesophageal cancers
IGF1	IGF1R	Transwell assay Wound healing	Breast cancer, sarcoma, multiple myeloma, lymphoma, melanoma
CSF1	CSF1R	Transwell assay 3D invasion *In vivo* invasion Intravital imaging	Breast, ovarian, endometrial, prostate and gastric cancers and leukemia
VEGFA and VEGFC	VEGFR1-3	Transwell assay 3D culture	Melanoma, prostate cancer, sarcoma, meningioma and leukemia

Table II. Types of directed cellular migration

	Unicellular migration		**Multicellular migration**	
Movement type	Amoeboid	Mesenchymal	Colective or chain migration	Streaming
Cellular type	WBC Tumor cells	Fibroblasts Tumor cells	Cells involved in gastrulation, wound healing and cancer	Tumor cells Cells involved in development of neural crest
Microenvironment factors influencing migration	Chemokine gradient and growth factors	Chemokine gradient and growth factors	Chemokine gradient and growth factors, extracellular matrix reorganization	Chemokine gradient and growth factors, extracellular matrix reorganization
Change of cellular morphology	Amoeboid to mesenchymal	Mesenchymal to amoeboid, mesenchymal to colective	Colective to unicellular migration	Undetermined
Processes involving cellular movement	Immune response Tumor invasion	Development Immune response Tumor invasion	Development and morphogenesis Neovascularization Tissue healing Tumor invasion	Development Tumor invasion
Cancer type	Breast and prostate cancer, melanoma	Breast and prostate cancer, melanoma, lung carcinoma	Breast, prostate, lung, colorectal cancer, melanoma and squamous carcinoma	Breast cancer
References	7-15	7, 16, 17	7, 18-24	25-29

In this study, we evaluated the capacity of inducing chemotaxis on a tumor cell line – SK-BR3 breast adenocarcinoma. This cell line expresses epidermal growth factor receptors (EGFR), so that we used epidermal growth factor (EGF) as chemotaxis agent.

MATERIALS AND METHODS

SK-BR3 cell culture

For the SK-BR3 cell line, the producer recommends the complete culturing medium, which contains ATCC-formulated McCoy's 5a Medium Modified, supplemented with 10% Fetal Calf Serum (FCS). Subculturing is recommended to be 1:2, medium replacement 2-3 times/week. Cells are expanded in adherent culture plates, in cell incubators with humidity and 5% CO_2.

Chemotaxia protocol

The protocol for cells seeding in chemotaxia slides was as follows:

- 10,000 cells in suspension in 50 µl complete culture medium were pipeted in the central channel;
- Cells were left to adhere 30 minutes in incubator;
- EGF was added in lateral chamber in concentration of 10 ng/µl;
- the chemotaxis plates were placed on the Holomonitor M4 and monitored for 24 hours in a time-lapse manner;
- images were obtained at 10 minutes interval and analyzed with Hstudio software.

The SK-BR3 cells were monitored using the Holomonitor M4 as follows: a. without any adhesion substrate, evaluating motility of native cells; b. in fibronectin-coated culture plates; c. in presence of EGF (chemotaxis inductor) on special slides. Results were analyzed using the HStudio software.

RESULTS AND DISCUSSION

SK-BR3 cells were monitored for 24 hours with Holomonitor M4. The images were taken every 30 minutes and are represented as holograms of cultured tumor cells, adherent to the plastic surface. The 3D images are represented based on the occupied area and cellular height. Depending on the 3D image of the recorded event, the device can provide information related to cellular viability.

Figure 1 shows the 3D holographic aspect of SK-BR3 cells at moments 1, 50 and 99 from the 24-hours time-lapse. After 24 hours of continuous monitoring, the focus of the device becomes less accurate, so the experiment was stopped, also this is a transitory phenomenon.

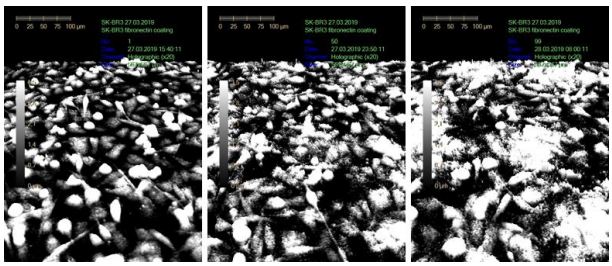

Fig.1. Time-lapse monitoring of SK-BR3 cells. Laser profilometry using Holomonitor M4. SK-BR3 were monitored for 24 hours in fibronectin-coated 6-well cell culture plates, images taken every 30 minutes. Ob. 20x

SK-BR3 tumor cells were first verified from the morphological point of view when cultured on semisolid matrices, such as fibronectin. Cells were seeded at a cellular density of 10,000 cells/cm^2 and monitored in optic microscopy for at least 24 hours before adding chemotactic substance.

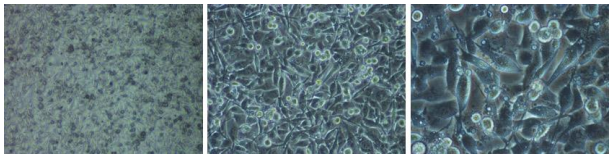

Fig.2. Morphological aspects of SK-BR3 cells cultured on fibronection-coated plates, optic microscopy, Ob. 4x, 10x, 20x.

In Figure 3, SK-BR3 cells are monitored with Holomonitor M4 while being cultivated in chemotaxia plates, in presence of EGF. The figure presents moments 1, 50 and 97 from the time-lapse recording. For further data interpretation we used the HStudio software, which can provide data regarding directed cellular motility.

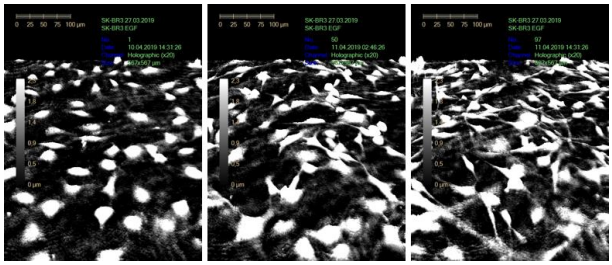

Fig.3. Time-lapse monitoring of SK-BR3 cells moving towards EGF gradient in fibronectin-coated chemotaxis plates. Holomonitor M4 images, Ob. 20x.

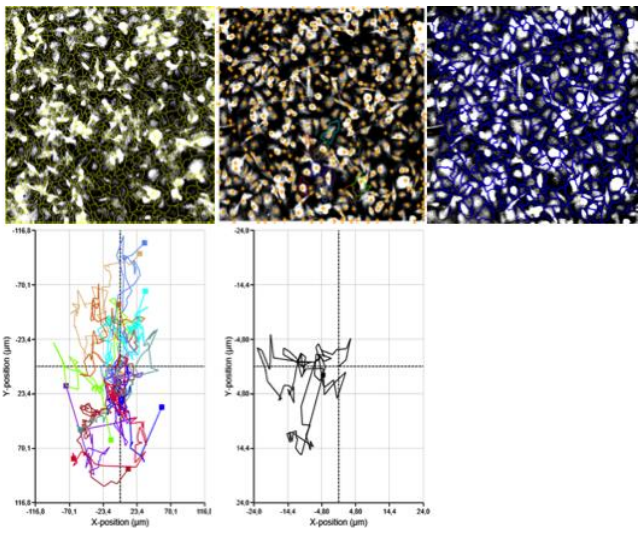

Fig.4. Motility graph of SK-BR3 cells represented for 10 cells (left panel) and average cellular population (right panel) without chemotactic factors, monitored in chemotaxis microplates fibronectin-coated.

The biaxial movement of cells is represented in Figure 4. Individual movement of 10 cells is represented on the left panel, while the average cell movement is represented on the right panel. The above images are automatically

generated by the HStudio software after identification of each holographic element as a cell. Biaxial representation of cellular movement and motility shows a disorganized pattern, but the average motility is clearly oriented towards the left part of the starting point.

When using the chemotaxia slides, the cells have a more directed movement in presence of EGF, whicle the average cell graph (right panel) shows a directness towards the positive end of the ox axis, which is towards the chemotactic factor (Figure 5).

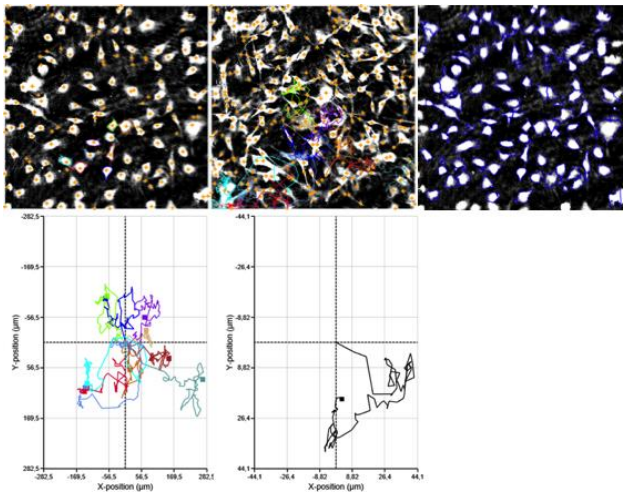

Fig.5. Motility graph of SK-BR3 cells represented for 10 cells (left panel) and average cellular population (right panel) with EGF as chemotactic factor, monitored in chemotaxis microplates fibronectin-coated.

Using the HStudio Holomonitor M4 specific software, we were able to evaluate motility, migration and migration speed for both SK-BR3 cells with or without EGF as chemotactic factor. On the left part of the Figure 6 we represented the parameters of the untreated cells, while the right panel represents the same parameters in presence of EGF gradient. All these parameters are quantitatively defined in Table III

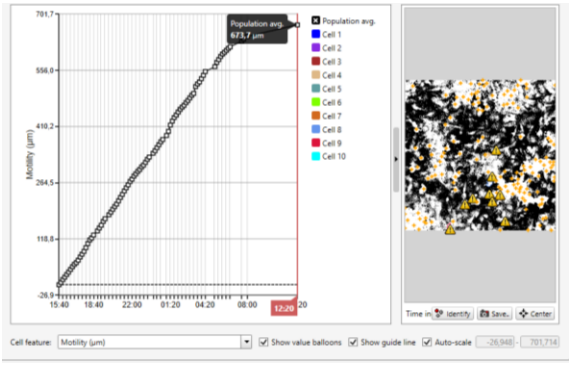

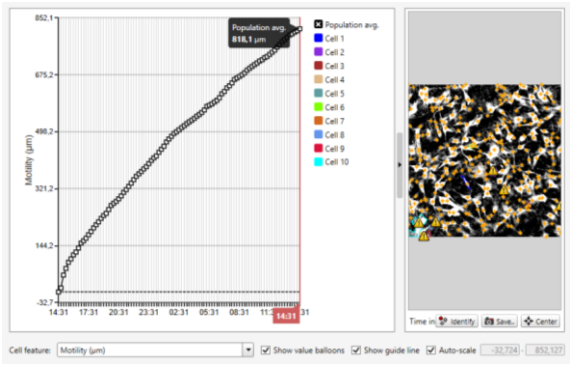

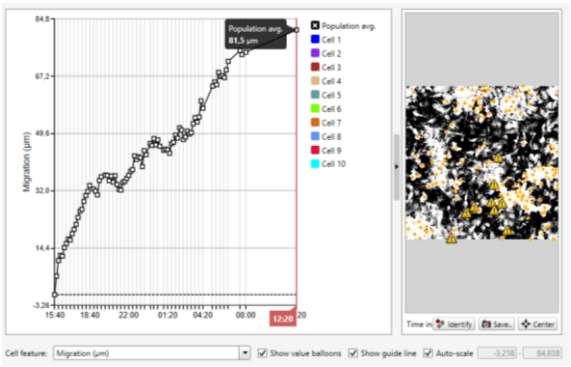

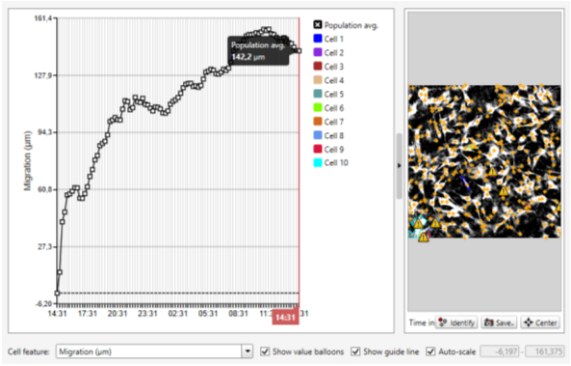

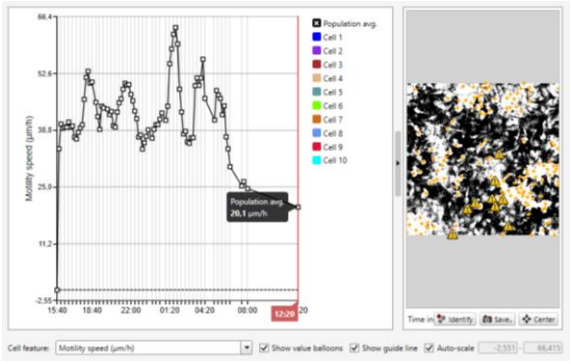

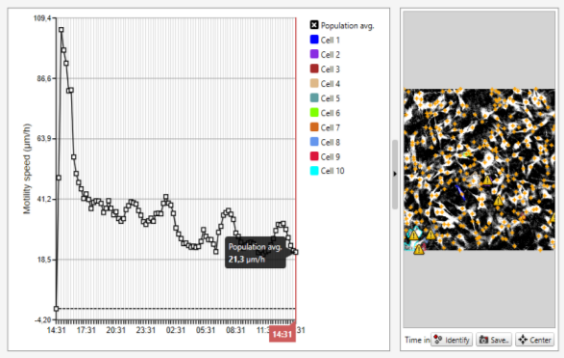

Fig.6. Graphical representation of parameters analyzed with HStudio software related to motility of native cells (left panel) and EGF – chemoatracted SK-BR3 tumor cells (right panel).

Table III. Comparative analysis of motility characteristics for SK-BR3 cells

	SK-BR3	SK-BR3 EGF
Motility (μm)	673.7	818.1
Migration (μm)	81.5	142.2
Migration speed (μm/h)	20.1	21.3

Considering the importance of chemotaxia in cancer, development of drug therapies targeting different steps in chemotaxis became a purpose of the recent scientific research. Recently, autonomous devices for monitoring chemotaxis, which can be implanted in vivo at tumor level, will help to a precise definition of the specific chemotactic signals involved in tumor cells migration [30]. Moreover, different compounds have been developed for a multitude of chemotactic factors, some of them being already in clinical use, others in clinical trials.

These studies present an *in vitro* model for studying the chemotactic ability of tumor cells (SK-BR3 breast cancer cell line) in the presence of EGF, a growth factor with chemotactic abilities. This is one of the first studies related to chemotaxia which involves holographic imaging using the Holomonitor M4.

Depending on the movement type, the cells thus monitored were included in a specific category of directed movement: unicellular, mesenchymal, which is very frequent in many cancers, including breast cancer. The migration speed (0.35 μm/min) (Table III) is also in accordance with the definition of the mesenchymal movement, according to Roussos ET *et al.* [4], which propose a range between 0.1-1 μm/min for this parameter.

CONCLUSIONS

This *in vitro* study is very important for invasion and tumor metastasis and provides a targeted image about these processes for SK-BR3 tumor cell line, mainly due to the investigation methods using Holomonitor M4 and holographic images analysis by HStudio software. These investigations could be further extended to analysis of other tumor cells and several different chemotaxis inducers.

Acknowledgement: This work was supported by the grant "Chimeric Antigen Receptor Targeted Oncoimmunotherapy with Natural Killer Cells (CAR-NK)", POC 92/09/09/2016, ID: P_37_786, MySMIS code: 103662.

REFERENCES

1. Justus CR, Leffler N, Ruiz-Echevarria M, Yang LV. In vitro cell migration and invasion assays. *J Vis Exp.* 2014; (88).
2. Tolde O, Gandalovičová A, Křížová A, Veselý P, Chmelík R, Rosel D, Brábek J. Quantitative phase imaging unravels new insight into dynamics of mesenchymal and amoeboid cancer cell invasion. *Sci Rep.* 2018; 8(1):12020.
3. Riol-Blanco L, Lazarevic V, Awasthi A, Mitsdoerffer M, Wilson BS, Croxford A, Waisman A, Kuchroo VK, Glimcher LH, Oukka M. IL-23 receptor regulates unconventional IL-17-producing T cells that control bacterial infections. *J Immunol.* 2010; 184(4):1710-20.
4. Roussos ET, Condeelis JS, Patsialou A. Chemotaxis in cancer. *Nat Rev Cancer.* 2011;11(8):573-87.
5. Zengel P, et al. μ-Slide Chemotaxis: a new chamber for long-term chemotaxis studies. *BMC Cell Biol* 2011; 12:21.
6. Biswenger V, et al. Characterization of EGF-guided MDA-MB-231 cell chemotaxis in vitro using a physiological and highly sensitive assay system. *PLoS One* 2018; 13(9):e0203040.
7. Friedl P, Wolf K. Plasticity of cell migration: a multiscale tuning model. *J Cell Biol.* 2010; 188:11–19.
8. Wolf K, et al. Compensation mechanism in tumor cell migration: mesenchymal–amoeboid transition after blocking of pericellular proteolysis. *J Cell Biol.* 2003; 160:267–277.
9. Wyckoff JB, Pinner SE, Gschmeissner S, Condeelis JS, Sahai E. ROCK- and myosin-dependent matrix deformation enables protease-independent tumor-cell invasion *in vivo*. *Curr Biol.* 2006; 16:1515–1523.
10. Nabeshima K, Inoue T, Shimao Y, Sameshima T. Matrix metalloproteinases in tumor invasion: role for cell migration. *Pathol Int.* 2002; 52:255–264.
11. Devreotes P, Janetopoulos C. Eukaryotic chemotaxis: distinctions between directional sensing and polarization. *J Biol Chem.* 2003; 278:20445–20448.
12. Veltman DM, Keizer-Gunnik I, Van Haastert PJ. Four key signaling pathways mediating chemotaxis in *Dictyostelium discoideum*. *J Cell Biol.* 2008; 180:747–753.
13. Annesley SJ, Fisher PR. Dictyostelium discoideum—a model for many reasons. *Mol Cell Biochem.* 2009; 329:73–91.
14. Wyckoff JB, et al. Direct visualization of macrophage-assisted tumor cell intravasation in mammary tumors. *Cancer Res.* 2007; 67:2649–2656.

15. Friedl P, Borgmann S, Brocker EB. Amoeboid leukocyte crawling through extracellular matrix: lessons from the *Dictyostelium* paradigm of cell movement. *J Leukoc Biol.* 2001; 70:491–509.
16. Sahai E, Marshall CJ. Differing modes of tumour cell invasion have distinct requirements for Rho/ ROCK signalling and extracellular proteolysis. *Nature Cell Biol.* 2003; 5:711–719.
17. Pankova K, Rosel D, Novotny M, Brabek J. The molecular mechanisms of transition between mesenchymal and amoeboid invasiveness in tumor cells. *Cell Mol Life Sci.* 2009; 67:63–71.
18. Gaggioli C, et al. Fibroblast-led collective invasion of carcinoma cells with differing roles for RhoGTPases in leading and following cells. *Nature Cell Biol.* 2007; 9:1392–1400.
19. Friedl P, Gilmour D. Collective cell migration in morphogenesis, regeneration and cancer. *Nature Rev Mol Cell Biol.* 2009; 10:445–457.
20. Valentin G, Haas P, Gilmour D. The chemokine SDF1a coordinates tissue migration through the spatially restricted activation of CXCR7 and CXCR4b. *Curr Biol.* 2007; 17:1026–1031.
21. Ilina O, Friedl P. Mechanisms of collective cell migration at a glance. *J Cell Sci.* 2009; 122:3203– 3208.
22. Wolf K, et al. Multi-step pericellular proteolysis controls the transition from individual to collective cancer cell invasion. *Nature Cell Biol.* 2007; 9:893–904.
23. Nabeshima K, et al. Front-cell-specific expression of membrane-type 1 matrix metalloproteinase and gelatinase A during cohort migration of colon carcinoma cells induced by hepatocyte growth factor/scatter factor. *Cancer Res.* 2000; 60:3364–3369.
24. Friedl P, Wolf K. Tube travel: the role of proteases in individual and collective cancer cell invasion. *Cancer Res.* 2008; 68:7247–7249.
25. Roussos ET, et al. Mena invasive (Mena^{INV}) promotes multicellular streaming motility and transendothelial migration in a mouse model of breast cancer. *J Cell Sci.* 2011; 124:2120–2131.
26. Giampieri S, et al. Localized and reversible TGFβ signalling switches breast cancer cells from cohesive to single cell motility. *Nature Cell Biol.* 2009; 11:1287–1296.
27. Kriebel PW, Barr VA, Parent CA. Adenylyl cyclase localization regulates streaming during chemotaxis. *Cell.* 2003; 112:549–560.
28. Kriebel PW, Barr VA, Rericha EC, Zhang G, Parent CA. Collective cell migration requires vesicular trafficking for chemoattractant delivery at the trailing edge. *J Cell Biol.* 2008; 183:949– 961.
29. Wyckoff J, et al. A paracrine loop between tumor cells and macrophages is required for tumor cell migration in mammary tumors. *Cancer Res.* 2004; 64:7022–7029.
30. Raja WK, Gligorijevic B, Wyckoff J, Condeelis JS, Castracane J. A new chemotaxis device for cell migration studies. *Integr Biol.* 2010; 2:696–706.

EVALUAREA *IN VITRO* A CHEMOTAXIEI CELULELOR TUMORALE SK-BR3 INDUSĂ DE EGF PRIN IMAGISTICĂ HOLOGRAFICĂ

REZUMAT

În acest studiu am evaluat capacitatea de inducere a chemotaxiei pe linia celulară tumorală SK-BR3, o linie celulară de adenocarcinom mamar. Această linie celulară a fost investigată morfologic, fenotipic și din punct de vedere al expresiei receptorilor pentru inductori ai chemotaxiei. Linia celulară SK-BR3 prezintă expresie de receptor pentru factorul de creștere epidermal (EGFR), în studiile noastre fiind utilizat EGF (factorul de creștere epidermal) ca factor inductor al chemotaxiei. Chemotaxia a fost studiată în plăci speciale pentru chemotaxie, utilizând un sistem de imagistică de tip holografic – Holomonitor M4.

Din punct de vedere morfologic, celulele tumorale ale celor 2 linii celulare investigate prezintă o formă poligonală, dimensiunile celulare sunt relativ mici, de aproximativ 15-20 μm. Efectele chemotactice la nivelul celulelor SK-BR3 induse de EGF au fost evidențiate prin evaluarea motilității, vitezei de deplasare, migrării și direcției de deplasare, parametri monitorizați timp de 24h. Celulele SK-BR3 cultivate pe fibronectină în prezența EGF, prezintă o motilitate crescută comparativ cu SK-BR3 fără factori de creștere (818,1 μm ± sd, respectiv 673,7 μm ±sd). Viteza de deplasare este mai mare de aproximativ 2 ori pentru SK-BR3 în prezenta EGF, migrarea este similară cu SK-BR3 fără factori, dar este unidirecțională.

Considerăm că acest studiu *in vitro* de o importanța deosebită în ceea ce privește invazia și metastazarea tumorală, care ne oferă o imagine țintită despre aceste procese pe linia celulară de adenocarcinom mamar SK-BR3, în special prin utilizarea Holomonitor M4 și analiza imaginilor holografice cu soft-ul Hstudio. Aceste investigații ar putea fi extinse în viitor prin studiul altor celule tumorale, în prezența altor factori inductori ai chemotaxiei.

Cuvinte cheie: chemotaxie, celule tumorale, Holomonitor M4, EGF